

**Improvement of the energy metabolism of
recombinant CHO cells by cell sorting for
reduced mitochondrial membrane potential**

Diplomarbeit zur Erlangung des akademischen Grades Diplom-
Ingenieur

durchgeführt am Institut für Angewandte Mikrobiologie an der
Universität für Bodenkultur in Wien, Österreich

eingereicht von Georg Hinterkörner

Wien, im Oktober 2008

Vorwort und Dank

Mein Dank gilt in erster Linie meiner Betreuerin, Prof. Nicole Borth, für einen interessanten Zugang zur Zellbiologie, für just immer genau die richtige Menge an Betreuung und Freiheit im Arbeiten und für Ihre Geduld.

Gelaufen wäre es trotzdem nicht ohne viele praktische Ezzes, ohne Einschulung in die Materie und ständig verfügbare Hilfe. Danke daher an Euch, Thomas, Helga, Martina, Kathi, Ingo, Wolfgang und Willi! Es war und ist mir eine Freude, mit Euch zusammenarbeiten zu können bzw dürfen.

Ich schätze mich glücklich, sowohl während des Studiums als auch während der Diplomarbeit viele nette und interessante Menschen kennen- und zu einem ganz kleinen Teil auch lieben gelernt zu haben. Rückblickend war das Studium der Lebensmittel- und Biotechnologie an der Universität für Bodenkultur nicht nur vom Thema, sondern auch aus einem sozialen Blickwinkel eine sehr gute Wahl.

Ohne meine Eltern hätte ich dieses Studium nicht so „schnell“ abschließen können. Auch wenn es manchmal schon zum Nicht-mehr-hören war, so hat mich doch der konstante, liebevolle Druck oft mit der notwendigen Motivation ausgestattet. Das sind Dinge, die erst später einleuchten.

Ihnen sei diese Diplomarbeit gewidmet.

Abstract

Immortalised mammalian cell lines such as Chinese Hamster Ovary (CHO) have great relevance to the industrial production of therapeutic proteins due to their posttranslational processing capacities, such as folding, assembly and glycosylation. Unfortunately, the indispensable process of immortalisation of such a cell line irreversibly and dramatically alters its patterns of energy metabolism. Glucose is mainly converted to lactic acid and is replaced by glutamine as the major nutritional factor. Thus, ammonia and lactate are released into the cell and the medium, starting to inhibit growth and induce apoptosis at a certain concentration, and finally interfere with the cell's biggest virtue and the reason, they are employed for production in the first place – their posttranslational machinery.

The present work exploits the heterogeneity of a cell population. Minor mutations or differences in several regulatory mechanisms lead to highly diverse metabolic patterns and efficiencies. By measuring the mitochondrial membrane potential of an antibody-producing CHO cell line with the fluorescent dye Rhodamine 123 and sorting out single cells with very low or very high signals using fluorescence activated cell sorting (FACS), it was possible to isolate subclones with improved or deteriorated metabolic characteristics in comparison to the parental cell line.

Growth, metabolic rates, antibody production and stability of the improved metabolisms were assessed in several batch cultures in different culture vessels. To get an insight into the genomic fundamentals of the different phenotypes of the subclones, they were analysed on the transcriptional level using microarray technology.

It could be shown that the subclones maintained their metabolic properties over a period of at least 6 months and also performed equally in different culture vessels, with slight differences in specific productivity. Transcriptional analysis elucidated that the improved characteristics could not be attributed to major changes in expression of key pathways in energy metabolism. In fact, upregulation of a part of the lipid metabolism, supplying the cell with precursors for hormones, vitamins and membrane components, might partly be responsible for the better performance.

This simple sorting procedure can be easily implemented in cell line development, leading to cell lines with less waste production and accelerated growth.

Zusammenfassung

Immortalisierte Säugetierzelllinien wie Chinese Hamster Ovary (CHO) Zellen sind aufgrund ihrer Fähigkeit zu komplexen posttranslationellen Modifikationen von Proteinen von großer Bedeutung für die biopharmazeutische Industrie. Der Weg hin zur immortalisierten Zelllinie ist jedoch unwiderruflich mit dramatischen Änderungen im Energiestoffwechsel der Zelle verbunden. Glukose wird hauptsächlich zu Laktat umgewandelt und in der Zelle als primärer Energieträger von der Aminosäure Glutamin abgelöst. Als Resultat gelangen Laktat und Ammonium in die Zelle und das Medium, was ab einer gewissen Konzentration zur Inhibition des Wachstums und zur Apoptose führt, und schlußendlich Einfluß auf die posttranslationelle Maschinerie der Zelle nimmt.

Die vorliegende Arbeit nützt gezielt gewisse Heterogenitäten innerhalb einer Zellpopulation aus. Unterschiede in intrazellulären regulatorischen Mechanismen führen zu einer Diversität im metabolischen Verhalten einzelner Zellen. Die Stärke des mitochondriellen Membranpotentials (MMP) wurde mithilfe eines MMP-abhängigen fluoreszenten Mitochondrienfarbstoffes (Rhodamine 123) sichtbar gemacht und mit fluoreszenz-aktiviertem Zellsorten (FACS) gemessen. Subklone mit besonders niedrigen oder besonders hohen Fluoreszenzintensitäten wurden isoliert, welche im Vergleich zur Mutterzelllinie verbesserte beziehungsweise verschlechterte Stoffwechseleigenschaften aufwiesen.

Wachstum, metabolische Raten, Antikörperproduktion und Stabilität der veränderten Klone wurden in mehreren Batch-Kulturen in verschiedenen Kultivierungssystemen analysiert. Auch eine Transkriptionsanalyse mittels Microarray-Technologie wurde durchgeführt.

Es konnte gezeigt werden, daß die verbesserten Eigenschaften über mehr als 6 Monate stabil und auch von der Art der Kultivierungssysteme unbeeinflusst blieben. Die Transkriptionsanalyse zeigte, daß in den vorliegenden verbesserten und verschlechterten Subklonen keine großen Veränderungen in der Transkription von Schlüsselgenen im Energiestoffwechsel vorlagen. Eine positive Regulierung eines wichtigen Teiles des Fettstoffwechsel, welcher die Zelle mit Vorläufern für Hormone, Vitamine und Membranbauteile versorgt, könnte jedoch den entscheidenden Ausschlag gegeben haben.

Es konnte eine simple, leicht anwendbare Technologie zur schnellen und frühen Anwendung in der Zelllinienentwicklung dargestellt werden.

INTRODUCTION.....	7
Energy metabolism of mammalian cell lines <i>in vivo</i> (according to Berg JM et al., 2007) ...	7
Glycolysis.....	7
Tricarboxylic acid cycle (TCC).....	8
Oxidative phosphorylation	9
Metabolism of glutamine	9
Metabolism of mammalian cell lines <i>in vitro</i> and immortalized mammalian cell lines	10
Influence of ammonia on protein glycosylation.....	10
Strategies for an improved efficiency of cellular metabolism	11
Fluorescence activated cell sorting (FACS).....	12
Principles	12
Instrumentation.....	13
Cell sorting	14
Rhodamine 123 as a probe for analysis of mitochondrial membrane potential (MMP)..	14
Transcriptional analysis	15
What to do with microarray data?	17
Kyoto Encyclopedia of Genes and Genomes (KEGG)	18
OBJECTIVES	19
MATERIALS AND METHODS	21
Cell culture	21
Batch experiments	21
Viability and cell count	22
Monitoring of Rhodamine 123 fluorescence.....	22
Mathematical equations.....	22
Haemocytometer	22
Coulter counter	23
Specific growth rate	23
Cumulative cell days (CD).....	24
Specific metabolic rates (qi).....	24
Cell sorting	24
Preparation of the cells	24
Sorting	25
Quantitative hIgG ELISA.....	26

Transcriptome analysis of sorted subclones	27
Isolation of total RNA	27
Processing of isolated RNA	27
Hybridisation, scanning and analysis of the cDNA microarrays	28
RESULTS.....	29
Cell sorting	29
Batch cultures	30
Batch cultures in roller bottles	30
Growth performance	31
Glucose uptake rates.....	31
Lactate production rates	32
Glutamine uptake rates.....	33
Specific mAb productivity	34
Summary	34
Batch cultures in spinner flasks.....	35
Growth performance	36
Specific glucose uptake	36
Specific lactate production	37
Specific glutamine uptake	37
Specific mAb productivity	38
Rhodamine 123 fluorescence	39
Summary	39
Transcriptional analysis.....	41
Metabolism.....	42
Glycerophospholipid metabolism:	42
Oxidative Phosphorylation:.....	43
Synthesis and degradation of ketone bodies & Steroid biosynthesis:.....	43
Sphingolipid metabolism:	45
Genetic information processing	46
Environmental Information Processing.....	46
Cellular Processes	46
DISCUSSION	48
CONCLUSION	55

LITERATURE 56

Introduction

Biopharmaceutical production of many therapeutic proteins depends on protein folding and glycosylation capabilities of continuous mammalian cell lines. However, most immortalised mammalian cell lines show a severe disorder in their glucose metabolism. Unlike in their tissue of origin, the cells metabolise glucose to pyruvate and further to lactate, by which NADH, emerging from glycolysis, is regenerated to NAD⁺. Since the energy gain from the glycolytic pathway is very small, the cells mainly infiltrate glutamine into the tricarboxylic acid cycle for generation of ATP in the respiratory chain. Metabolism of one mole of glutamine, however, releases two moles of ammonia into the cytoplasm. Besides its toxic effect, high ammonia concentrations are known to interfere with the glycosylation machinery, especially terminal sialylation, which is the very essence of why mammalian cell lines are employed in the biopharmaceutical industry in the first place.

Energy metabolism of mammalian cell lines *in vivo* (according to Berg JM et al., 2007)

Glucose as the main energy source enters the mammalian cell via a family of facilitative glucose transporter proteins (GLUTs). Driving force of the transport process is the glucose concentration gradient between the medium and the cytoplasm. So far 13 different GLUTs have been identified and assorted into three classes regarding substrate specificity, kinetics and – partly – localisation of a functionally important glycosylation site. Glucose transport against a concentration gradient, as it is necessary in kidney and small intestine tissue, is allowed by another family of transporter proteins, the sodium-dependent glucose transporter. They utilize a Na⁺ gradient provided by Na⁺-K⁺ ATPase pumps for the transport process (Wood and Trayhurn 2003). However, Chinese hamster ovary cells (CHO), as subject to this thesis, utilize GLUTs for glucose transport.

Glycolysis

The glycolytic, or Embden-Meyerhof pathway, is a sequence of enzymatically catalysed reactions turning the C₆-body glucose into two C₃-bodies of pyruvate, which is common in basically most glucose consuming organisms. These reactions sum up to an energy gain of 2 Mol adenosine triphosphate (ATP) and 2 Mol NADH out of 1 Mol of glucose. The fate of

pyruvate is uncertain and dependent on organism and environment. Amongst others, it can be reduced to lactate as in lactic acid forming microbes or in strained skeletal muscle, or converted to ethanol and further to acetic acid. Aerobic organisms, including mammalian cell lines, decarboxylate pyruvate to Acetyl-Coenzyme A, which is then completely oxidised to CO₂ and water via the tricarboxylic acid cycle and the oxidative phosphorylation inside the mitochondria, generating ATP.

The glycolytic pathway generally comprises three stages. Stage 1, which is the conversion of glucose into fructose 1,6-bisphosphate, consists of three steps: a phosphorylation, an isomerization, and a second phosphorylation reaction. Stage 2 is the cleavage of the fructose 1,6-bisphosphate into two three-carbon fragments and in stage 3, ATP is harvested when the three-carbon fragments are oxidized to pyruvate.

Reactions of the glycolysis are located in the cytosol.

Tricarboxylic acid cycle (TCC)

The tricarboxylic acid cycle (Krebs or citric acid cycle) is the center point of a cell's energy metabolism. Not only is the cell able to metabolise basically any substrate that can be turned into an acetyl group or dicarboxylic acid, but it can also extract precursor molecules for assembly of necessary building blocks like nucleotides, amino acids, cholesterol, etc. The TCC is located in the matrix of the mitochondria.

Pyruvate, as the product of glycolysis, enters the mitochondrion via the pyruvate carrier which functions as an antiporter. Inside the mitochondrion, pyruvate is decarboxylated to an acetyl group and bound to coenzyme A. This reaction is irreversible and the link between glycolysis and TCC, thus making it an important regulatory point in the cell's metabolism.

Acetyl coenzyme A enters the TCC by condensation with oxalacetate, forming a C-6 body (citric acid). Citric acid is isomerised to isocitrate and then twice decarboxylated first to α -ketoglutarate and then to succinate. Succinate is then regenerated to oxalacetate in a few steps. Two carbon atoms are oxidated to CO₂, three hydride ions are transferred to nicotinamide adenine dinucleotide (NAD⁺) and one pair of hydrogen atoms is transferred to flavine adenine dinucleotide (FAD). Electrons from NADH and FADH₂ are then transferred stepwise to O₂ in the process of oxidative phosphorylation driving the production of ATP.

Oxidative phosphorylation

Oxidative phosphorylation is the process in which ATP is formed as a result of the transfer of electrons from NADH or FADH₂ to O₂ by a series of electron carriers. The process takes place in the matrix of the mitochondria.

Electrons from NADH from glycolysis, fatty acid oxidation and mainly the TCC are transferred to O₂ by three transmembrane protein complexes, which are the NADH-Q oxidoreductase, the Q-cytochrome *c* oxidoreductase and the cytochrome *c* oxidase. Several oxidation/reduction centers inside these proteins, such as quinones, iron-sulfur groups, heme groups or copper ions allow the uptake of electrons.

Upon reception of electrons, these protein complexes pump protons to the intermembrane space of the mitochondrion, thus creating a pH-gradient between the matrix and the intermembrane space. Backflow of protons through the F₀ channel subunit of the ATP synthase is then used by the F₁ subunit to generate ATP out of ADP and P_i. Backflow of at least 3 protons is necessary to allow generation of 1 molecule of ATP.

Another transmembrane complex, the succinate-Q reductase, transfers electrons from FADH₂ to quinone. The TCC enzyme succinate dehydrogenase is part of the complex, which by converting succinate into fumarate generates the FADH₂. Since this complex does not function as a proton pump, less ATP is generated from FADH₂ than from NADH.

Metabolism of glutamine

Free amino acids are the products of digestion of proteins. They are either used as building blocks for protein synthesis or transformed into a series of metabolic intermediates which are acetyl-CoA, acetoacetyl-CoA, succinyl-CoA, α-ketoglutarate, pyruvate, fumarate and oxalacetate. These intermediates are then either transformed into glucose via gluconeogenesis or infiltrated into the tricarboxylic acid cycle.

Glutamine is hydrolysed to glutamate and NH₄⁺ by the enzyme glutaminase and then oxidatively deaminated to α-ketoglutarate, which enters the TCC. In terrestrial vertebrates, the accumulating ammonia is transformed into urea in the liver. Alanin and glutamine – by amination of pyruvate or glutamate – serve as acceptor molecules for ammonia.

Metabolism of mammalian cell lines *in vitro* and immortalized mammalian cell lines

For keeping up metabolism in multicellular organism, an interaction of several differentiated tissues is needed. Not every cell type is capable to perform every metabolic pathway in an organism. Parts of the metabolic reactions are transferred to the liver and kidney, like gluconeogenesis and lactate metabolism, catabolism of fatty acids or production of urea. The isolated cell type grown in a culture dish is therefore limited to its own metabolic capabilities. Immortalised, continuous cell lines, like Chinese Hamster Ovary (CHO) or hybridoma cell lines show severe disorders in their energy metabolism. 15 to 20% of the glucose enters the pentose phosphate pathway, residual glucose enters the glycolytic pathway. 0 to 5% of the resulting pyruvate is converted to acetyl-CoA and enters the TCC, the rest of the pyruvate is reduced to lactate by the enzyme lactate dehydrogenase.

Accumulation of lactate leads to acidification of the medium and can have an inhibitory effect on cell growth at a certain concentration that strongly varies between different cell lines. Additionally, this pathway leads to a very poor energy gain of only 2 mol ATP per mol glucose, compared to a theoretical 36 mol through complete oxidation in the mitochondria. Glutamine is therefore added to cell culture medium as main energy substrate for the cells, which nearly completely enters the TCC.

However, metabolism of glutamine includes, as described in a previous section, two deamination steps in the mitochondria, releasing ammonia into the mitochondrial matrix. Besides alkalisation of the mitochondria, ammonia can influence protein glycosylation patterns.

Influence of ammonia on protein glycosylation

Ammonia affects protein glycosylation simultaneously on several levels. Elevated levels of ammonia in the medium alkalise the cytoplasm, leading to a higher antennarity of N-glycans (Maiorella 1992, Valley et al. 1999).

An increased amount of ammonia both influences production of carbamoyl phosphate (CP), which is a precursor for uridine triphosphate (UTP), and increases formation of UDP-activated N-acetyl hexosamines (UDP-GNAc) by incorporation of ammonia at the step of

building glucosamine-6-phosphate (GlcN6P) from fructose-6-phosphate (Frc6P). UTP and GlcN6P are afterwards condensed to UDP-N-acetylglucosamine (UDP-GlcNAc). At elevated concentrations, UDP-GlcNAc has a higher flux into the Golgi apparatus using the nucleotide sugar transport system I, thus suppressing transport system II, which is used for transfer of CMP-N-acetylneuraminic acid (CMP-NANA or CMP-sialic acid). By blocking its transfer, the concentration of CMP-NANA in the cytoplasm increases, thus blocking its own synthesis pathway via feedback inhibition. Therefore, less CMP-NANA reaches the Golgi apparatus, leading to a reduced sialylation of N-glycans (Valley et al. 1999).

Strategies for an improved efficiency of cellular metabolism

Strategies for improving the efficiency of metabolism in continuous mammalian cell lines comprise different approaches through medium formulation, clone selection, process setup and genetic engineering.

One approach was to substitute glucose with galactose, fructose or mannose (Altamirano et al. 2000). Specific sugar uptake rates for galactose and fructose were reduced to about 25% of the corresponding values of glucose and mannose, which showed a similar performance. Specific lactate production rates for cell cultures grown in galactose- or fructose-containing medium drastically dropped to values around 22% of the corresponding rates for glucose uptake, indicating complete oxidation of a major part of the supplied hexose. Growth rates and final cell densities decreased to 50-70% when compared to cell cultures in glucose- or mannose-containing medium. Glutamine uptake rates were increased and in spite of the lower cell densities, the absolute ammonium concentration was also elevated compared to glucose and mannose cultures. Replacement of glutamine by glutamate was more successful, leading indeed to lower cell counts for both glucose and galactose as sugar supply, but at the same time severely reducing release of ammonia in the medium.

Choice of the cultivation system and process parameters can also have an impact on the metabolism of continuous mammalian cell lines. (Europa et al. 2000) reported a metabolic shift to severely reduced metabolic rates when starting a continuous culture out of a fed batch with a low glucose feed, when compared to the same continuous process started from a batch culture.

Variation of process parameters like dissolved oxygen tension, pH and temperature has also shown an impact on cell growth and metabolism and also specific productivity in recombinant cell lines (Bollati-Fogolín et al. 2005, Trummer et al. 2006).

Genetic engineering approaches to specifically influence cellular metabolism generally aim at single target enzymes in metabolic pathways, such as the enzyme lactate dehydrogenase (LDH). LDH catalyses the reduction of pyruvate to lactate. A knock-out of one allele of the LDH gene has been done before and led to a reduction of lactate formation and an extended life span of the cell culture, thus elevating end cell concentration in the culture (Chen et al. 2001). Targeting of anti-apoptotic genes such as Bcl-2, Bcl-xL, Aven and the adenoviral gene E1B-19K resulted in reduced lactic acid formation and extended life spans (Arden and Betenbaugh 2004).

In development of cell lines, subcloning of cells and analysis of resulting subclones to find a suitable production or host clone is a common process. This process indirectly makes use of the fact that there exists a large heterogeneity among cells within a population, as far as their metabolism, reproductive machinery and protein expression capabilities are concerned. This can be due to mutations, change of epigenetic silencing or other regulatory mechanisms inside the cell.

If these cells, that have changed and improved properties, can be made visible to a high-throughput technology like fluorescence activated cell sorting (FACS), and sorted from the rest of the population, an optimisation protocol would emerge, that can be applied for directed improvement at a very early stage in cell line development.

Fluorescence activated cell sorting (FACS)

Principles

Fluorescence activated cell sorting (FACS) allows determination of various parameters of cells, cellular components or other particles of a certain size, that can be suspended in a fluid, at a very high number per unit of time. Particles can be measured individually by consecutively passing a laser in a fluid stream. Reflected or emitted fluorescent light is then converted to digital signals by photodiodes or photomultipliers, and analysed on a computer.

High throughput and a steadily growing range of fluorogenic substances with highly specific targeting capabilities and make FACS a powerful analytical technology. Today, FACS is applied in both clinical and research laboratories for cell cycle and apoptosis analysis, immunofluorescence, analysis of protein or DNA content, assaying secretion, determination of the viability of cells or for diagnosis of diseases like leukemia.

Additionally, FACS allows to electrostatically sort single cells with predefined characteristics out of a cell population.

Instrumentation

Basic parts of a flow cytometer are a light source (laser) combined with an optics system to direct and focus the beam, a fluidics system to create a laminar particle stream, an electronic system for capturing light signals and converting them to digital signals, and a computer equipped with the appropriate software for analysis.

Flow cytometers are equipped with one or more lasers, usually one or a combination of Argon ion, Helium/Neon or Krypton lasers. The emitted intense, single wavelength light with a narrow diameter allows both specific excitation of fluorochromes and centering the laser beam on the fluid stream. Focusing is done with a combination of lenses.

The particle stream is injected into a hull or sheath stream, both passing a narrow aperture of about 50 - 400 μm , which accelerates the combined streams and focuses the particles (cells, etc) in the center of the stream (*hydrodynamic focusing*).

Light signals emerging from the intersection point of laser beam and fluid stream are focused on and captured by photodetectors (photodiodes, photomultiplier tubes). A series of filters split the emerging light into different fractions according to their wavelength, with each of the fractions hitting their own detector. The photodetectors convert the light into digital signals, which are then sent to a computer for analysis.

Several different parameters can be measured simultaneously for each cell separately. The forward scatter signal (FSC) gives information on the size of the cell in comparison to the rest of the population. The side scatter signal (SSC) is dependent on both the condition of the cell's surface, size and internal structure. Both signals are defined as light of the same colour as the original laser beam, with FSC only bent to a small angle and SSC bent to 90°. Additionally, several fluorescence channels (FL1,2,3,...) can be measured, dependent on type and number of excitation wavelengths available.

Data can be rendered either as histograms, dot or contour plots, with regard to the desired information.

Cell sorting

With the according equipment, a flow cytometer is capable of separating cells, that meet predefined characteristics, from the rest of the cell population, which is referred to as cell sorting. Cells can be deposited in different culture vessels, either individually or in bulk.

Therefore, the instruments injection head, where the particle and the sheat stream are merged, is brought to a constant and fast vertical oscillation by a piezo-electric element. This oscillation leads to a break-off of the fluid stream after the intersection with the laser beam. Precise measurement of the distance between the intersection and break-off allows electrostatical charging of the drop that contains the desired cell. Then, oppositely charged metallic plates deflect the drop into the desired culture vessel. To eliminate uncertainties in timing, the drops immediately before and after the desired drop are usually sorted as well.

Rhodamine 123 as a probe for analysis of mitochondrial membrane potential (MMP)

Rhodamine 123 (Fig. 1), a cationic, lipophilic fluorochrome at physiological pH, is able to stain mitochondria directly and provides low-background, green-fluorescent images of mitochondria. Absorption and emission maxima are at wavelengths of 507 and 529 nm respectively.

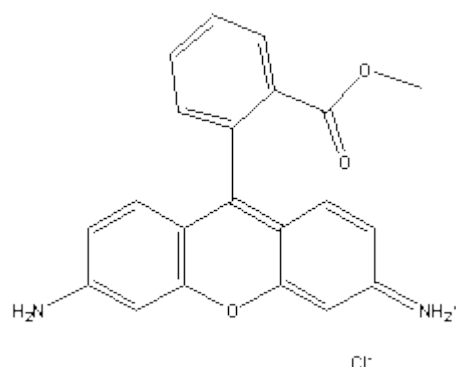


Fig. 1: chemical structure of Rhodamine 123

The use of this dye enables the selective staining of mitochondria in living cells and gives a good measure of mitochondrial activity when quantified by flow cytometry (Johnson et al. 1981). Because of their negative membrane potential, mitochondria accumulate lipophilic cations (Chen 1989) like Rhodamine dyes. The positive charge allows the probe to pass through the cell membrane and accumulate in the negatively charged environment of the inner mitochondrial membrane. There the lipophilic part of the probe assures retention in the membrane lipid bilayer (Keij, Bell-Prince and Steinkamp 2000). Therefore the extent of uptake reflects the redox potential across the mitochondrial membrane (Johnson et al. 1981). The mitochondrial membrane potential (MMP) measured by Rhodamine 123 corresponds to the glucose uptake rate, which, for a given cell line, corresponds in turn to the glucose concentration in the medium (Borth, Kral and Katinger 1993).

Unfortunately, Rhodamine 123 also shows photoinduced bleaching (Chen 1989) and non-coherent behaviour (Salvioli et al. 1997).

Transcriptional analysis

An in-depth analysis of intracellular procedures of cells with different behaviour is highly desirable, not only in disease research but - in the present work - also for CHO subclones that exhibit differences in their energy metabolism. Both the amount of mRNA of certain genes and the level of actually translated proteins present in a cell at a certain timepoint are of particular interest to a more profound understanding of cellular processes.

Transcriptional profiling (*genomics*), that comprises only a limited number of well-known genes can be done with rather time-consuming methods such as Northern Blot and real-time PCR. To get information on the interaction of genes in a cell resulting in a different phenotype, transcriptional levels of the whole genome or at least a very wide variety of genes have to be analysed (*functional genomics*). Microarray technology allows a simultaneous quantitative transcriptional analysis of a large number of genes, which in recent years ranged up to whole genomes.

The principle of mRNA analysis with microarrays is based on hybridisation of isolated RNA to homologous sequences immobilised on the array. The isolated RNA is *in vitro* reverse-transcribed to cDNA and again transcribed to cRNA, with a parallel incorporation of fluorescently labelled nucleotides. The more mRNA of one gene has been present earlier in

the cell, the more RNA (or cDNA) will hybridise to the according spot on the array, thus increasing brightness of the spot when scanned with a laser and allowing quantification. Direct comparison of mRNA levels on one array (e. g. comparison to healthy tissue of the same type, a non-transformed cell line, cells from another tissue type, or, like in the present case, the parental cell line) employs a two-dye strategy. RNA from sample and reference tissue or cell culture are labelled with different dyes; incorporation of red and green fluorescent cyanine-labelled nucleotides at transcription from cDNA to cRNA is rather common. cRNA from both sample and reference will bind to the corresponding spot on the array slide according to their present amount. Thus, the colour of the fluorescent signal of one spot will shift towards red or green if there is a difference in transcription of this gene between sample and reference tissue. Since efficiency of dye incorporation is not the same for cyanine dyes, resulting variations have to be filtered out at the point, where the information is drawn from the slides (*feature extraction*). Two-dye experiments allow calculations of gene-specific transcriptional fold changes between sample and reference. Due to the possibility of biological variations from one culture experiment to another, the reference (or standard) should be picked carefully.

Dependent on the type of microarray, cDNA (~1 kbp), PCR products (200 – 400 bp) or oligonucleotides (20 – 60 bp) are spotted on a surface made of glass, plastic or silicone, with each spot showing distinct homology to one specific gene. The smaller the size of the spots, which is dependent on the type of array and technology, the more spots can be dotted and the more genes can be analysed simultaneously. Currently, commercially available microarrays (from Affymetrix, Agilent, Clontech,...) reach a spot diameter of only 5 µm and can represent more than one genome on a single glass slide.

The microarray platform used for the present work was purchased from Agilent, USA. About 22.000 different 60-mer oligonucleotides are spotted on one glass slide, representing about two thirds of the mouse (*Mus musculus*) genome. Since the genome of the Chinese Hamster (*Cricetulus griseus*) has not yet been thoroughly sequenced, mouse arrays are often used for transcriptional analysis of CHO cells. Reliability of cross-species hybridisation experiments has been evaluated (Ernst et al. 2006).

What to do with microarray data?

Interpretation of the sheer amount of data, that has been drawn from transcriptional analysis endorsed by microarray technology, presents a big challenge to the experimenter. Extraction of fluorescent signal data from the array slide, compensation of variations in dye incorporation, determination of correctly and incorrectly stained spots and alignment of the signals to the underlying gene identity file is usually done by programs provided by the array supplier, in the present case the program was *GeneSpring* (Agilent, USA). The output usually consists of gene lists containing gene IDs, raw fluorescent signal data and – if a standard has been used – information on transcriptional fold change in comparison to the standard. The researcher is left to make sense of these gene lists.

Several problems arise at this point. It is likely to get a list of genes with significant fold change but they might all lack a unifying biological theme, which leaves interpretation to the knowledge of the researcher. Also, change in transcription of one single gene, even if abundant, is seldom responsible for significant alterations in cellular behaviour or morphology. It is more likely, that a series of cooperating genes or genes of one specific cellular pathway contribute to phenotype changes. Fold changes of these genes might even lie beyond thresholds defined by the inherent background noise of microarray experiments, thus hiding them from the interpreter's attention. Additionally, thinking of e. g. inhibitory kinases, both up- and downregulation of genes might result in a better flux, in an enhancement of one specific pathway or vice versa.

Gene set enrichment analysis (GSEA) allows interpretation of microarray data based on gene sets (Subramanian et al. 2005). These gene sets can consist of genes encoding products in one metabolic pathway, genes that are located in the same cytogenetic band, or share the same arbitrarily determined category. They can be self-designed or retrieved from published biochemical pathways like KEGG (*Kyoto Encyclopedia of Genes and Genomes*) Pathway. GSEA is a suitable tool to compare expression profiles of two samples (e. g. sample and reference). It sorts the gene list derived from a microarray experiment into a ranked gene list L along a user-defined metric, which in this present case was the transcriptional fold change (i. e. the difference between sample and reference in amount of mRNA of any gene transcribed in the cell at a certain timepoint). One or more predefined gene sets S, which were in this work derived from KEGG, are then compared to the ranked gene list L one at a time. It is then determined whether the members of S range at the top or bottom of L or if they are equally distributed along L. These three cases would imply up-, down- or no regulation at all

of the gene set. GSEA calculates a so-called enrichment score, which gives an impression on the magnitude of transcriptional regulation of the gene set, and indicates up- or downregulation with either prefixes “-“ or “+”. The GSEA output is statistically backed up by multiple hypothesis testing and calculation of a false discovery rate (FDR). For more information on the mathematical part of this matter, the author would like to refer to the publication mentioned at the beginning of this paragraph.

Kyoto Encyclopedia of Genes and Genomes (KEGG)

KEGG is a database of biological systems, consisting of genetic building blocks of genes and proteins (KEGG GENES), chemical building blocks of both endogenous and exogenous substances (KEGG LIGAND), molecular wiring diagrams of interaction and reaction networks (KEGG PATHWAY), and hierarchies and relationships of various biological objects (KEGG BRITE). KEGG provides a reference knowledge base for linking genomes to biological systems and also to environments by the processes of PATHWAY mapping and BRITE mapping.^a Several more features have recently been added like KEGG GLYCAN or KEGG DRUG. For further general information, the website refers to the publications of Kanehisa and Goto 2000, Kanehisa et al. 2006 and Kanehisa et al. 2008.

For analysis of microarrays in the present work, the pathway section of KEGG was used. KEGG PATHWAY divides data on biological interactions and cellular networks into the sections *metabolism*, *genetic information processing*, *environmental information processing*, *cellular processes* and *human disease*, each of them consisting of numerous subcategories. The section “human disease” was excluded for analysis.

^a From: <http://www.genome.ad.jp/kegg>

Objectives

As mentioned before, immortalized mammalian cell lines show disorders in their energy metabolism compared to normal tissue. Glucose is mainly converted to lactate with low energy gain, making it necessary to supplement glutamine to the medium. Upon its utilisation, glutamine releases ammonia into the cell, thus influencing the glycosylation machinery, the unique ability of mammalian cells. A renunciation from glutamine as main energy substrate to a more efficient metabolism of glucose would be desirable. In the present work, the possibility of implementing this improvement of cells into cell line development is discussed.

The usual way of establishing a new production cell line is to subclone the cells and screen the resulting clones for productivity and growth characteristics. The number of subclones is then narrowed down to allow re-screening in cultivation systems similar to the production plant within a reasonable period of time (e. g. small-scale bioreactors). In the end, one production clone is selected and process development begins.

The present work aims at an early selection of subclones that already have an improved metabolism – i. e. lower specific glucose (qGlc) and glutamine uptake (qGln) and lower lactic acid formation rates (qLac) – compared to the rest of the cell population, using fluorescence activated cell sorting (FACS) as high-throughput technology. The mitochondria as key elements in cellular metabolism were selected as targets for fluorescent labelling. The green-fluorescent, cationic, lipophilic dye Rhodamine 123 specifically stains the mitochondrial membrane and exhibits quenching of its fluorescent signal according to the force of the membrane potential (Chen 1989, Baracca et al. 2003).

Previous work on the matter has indicated a close relation between glucose concentration in the medium, specific glucose uptake rate in the cells and Rhodamine 123 fluorescence intensity (Borth et al. 1993). A CHO cell line, producing a monoclonal anti-HIV1 antibody was single-cell sorted for both low and high rh123 fluorescence intensity. Obtained subclones with low rh123 fluorescence signal showed a clear tendency towards reduced glucose consumption and lactate production rates, whereas subclones sorted on high fluorescence exhibited opposite characteristics. Subclones that differed the most from the parental cell line in their metabolic rates (entitled HR1 for *high Rhodamine* and LR2 for *low Rhodamine fluorescence*), were picked for characterisation in repeated batch runs in different cultivation

systems. Messenger RNA from both subclones and from the parental cell line was harvested in comparable growth conditions and growth phases for analysis of the transcriptome using a cross-species hybridisation approach on mouse oligo microarrays, which had been successfully established in the lab before (Ernst et al. 2006).

Materials and Methods

Cell culture

The cell line used, named CHO-2G12, was a recombinant Chinese Hamster Ovary (CHO) DHFR- cell line, producing the IAM2G12 human monoclonal anti-HIV1 antibody. Cells were cultured in serum-free DMEM/Ham's F12 (1:1) supplemented with 4 mM L-glutamine, 0.25 % soy peptone, protein free additive, 0.1 % Pluronic F68 and 1 μ M methotrexate (MTX). Cultivation experiments were carried out at 37°C in 125 ml spinner flasks (Tecne, USA) and 2000 ml roller bottles (Nunc, USA) pre-gassed with 60 and 120 ml of sterile-filtered CO₂ respectively to resemble a 7 % CO₂ atmosphere. To facilitate adaptation to the spinner flasks, an anti-clumping agent (Gibco, USA) was added at a concentration of 1:500.

Batch experiments

Characterisation of the sorted subclones was done in cultivation experiments in batch mode in 125 ml spinner flasks (Tecne, USA) with a maximum volume of 100 ml as well as in 2000 ml roller bottles at a maximum culture volume of 200 ml. Batch mode cultivations were started at a concentration of 2 x 10⁵ viable cells/ml. Cells were centrifuged at 170 g for 10 minutes, taken up in fresh prewarmed medium as described above and transferred to the spinner flask. Cell count, viability and concentrations of glucose, lactate and glutamine were determined daily, Rhodamine fluorescence and hIgG titer every second day. Additionally, samples for isolation of mRNA were drawn on days 2 and 3 of the batch phase. Concentrations of glucose, lactate and glutamine were determined using a YSI 7100 MBS multiparameter bioanalytical system (YSI Life Sciences, USA), content of human IgG was determined by quantitative ELISA.

A first characterisation of subclones that emerged from sorting experiments was done in T25 flasks under the same conditions as mentioned above. Samples were drawn on batch start and on the second day to determine cell count and glucose, lactate and glutamine concentrations. Promising subclones were evaluated further as described above.

Viability and cell count

Viability was determined with the trypan blue exclusion method using a hemocytometer (Bürker Türk, Germany), cell count by counting the cell nuclei in a Multisizer III (Beckman Coulter, USA) after treatment of the cell pellet with an aqueous buffer of 2 % (w/v) Triton X-100 and 100 mM citrate for at least 2 hours.

Monitoring of Rhodamine 123 fluorescence

Rhodamine 123 fluorescence intensity of the cells was monitored. Therefore, approximately 10^6 cells were transferred from the culture flasks into 10 ml vials and incubated with a stock solution of Rhodamine 123 [1 mg/ml] at a dilution of 1:100 for 15 min at 37°C. After incubation, cells were centrifuged at 170 g for 10 min, washed with PBS, spun down again and resuspended in 1 ml PBS. Cell suspensions were then transferred to FACS vials and analysed on a FACSCalibur (Beckton Dickinson, USA).

Mathematical equations

Haemocytometer

The density of living and dead cells and the total cell density were determined according to

$$X_i = \frac{\text{counts}_i}{n_s} \cdot d \cdot 1.2 \cdot 10^4 \text{ [cells/ml]}$$

The viability was calculated by

$$V = \frac{X_v}{(X_v + X_d)} = \frac{X_v}{X_i}$$

X ...cell density

V ...viability

X_v ...number of viable cells

X_d ...number of dead cells

- X_t ...total cell number
- i ...index variable: v-viable; d-dead; t-total
- n_s ...number of squares
- d ...factor for dilution sample
- 1.2 ...dilution factor for addition of trypan blue
- 10^4 ...number of squares [0.1 μ l] per ml

Coulter counter

The cell density was calculated according to

$$X_i = \frac{\frac{1}{S} \cdot \left(\sum_{i=1}^n counts_i \right) \cdot (c + e) \cdot b}{c \cdot a} \quad [\text{cells/ml suspension}]$$

- X ...cell density
- i ...index variable
- n ...number of counts
- a ...volume of cell suspension centrifuged [ml]
- b ...volume of lysis buffer
- c ...volume of incubated sample taken for measurement [ml]
- e ...volume of electrolyte
- S ...volume of sample counted

Specific growth rate

The specific growth rate μ for batch conditions is defined as the time dependent increase in cell number based on cell density.

$$\mu = \frac{\ln X_2 - \ln X_1}{t_2 - t_1}$$

- X_2 ...cell number at t_2
- X_1 ...cell number at t_1

(t_2-t_1) ...time interval between sampling timepoints

Cumulative cell days (CD)

Cumulative cell days is a mathematical tool for calculating the specific consumption rate and the specific production rate. It represents the area under the growth curve of a culture.

$$CD = \sum_{q=1}^n \frac{X_{b+1} - X_b}{\ln X_{b+1} - \ln X_b} \cdot (t_{b+1} - t_b) = \sum_{q=1}^n \frac{X_{b+1} - X_b}{\mu}$$

Specific metabolic rates (q_i)

The specific productivity and consumption rate were calculated as a function of cumulative cell days CD.

$$q_i = \frac{(c_n - c_i)}{\sum_{q=1}^n \frac{X_{b+1} - X_b}{\mu}} \text{ [ng/CD]}$$

c ...concentration of nutrient/product at sampling timepoint

Specific glucose consumption rate and specific lactate production rate, as well as the specific antibody production rate were calculated according to this equation.

Cell sorting

Preparation of the cells

Cells were single-cell sorted into 96-well plates. The 96-well plates were filled with 150 μ l of a 1:1 mixture of the above described medium and sterile filtered culture supernatant of the same cell culture, and spiked with 1:100 of a penicilline/streptavidine antibiotic mix. The plates and medium were warmed and preconditioned in an incubator in humidified atmosphere with 7 % CO₂ at 37 °C.

The Rhodamine 123 staining procedure was the same as for monitoring of the Rh123 signal during batch cultures, as described above. Shortly before the sorting process, 1:100 DAPI was added.

Sorting

Cell sorting was done on a FACSVantage (Beckton Dickinson, USA) equipped with Pulse Processing, Sort Enhancement Module and Automatic Cell Deposition Unit. A 5 W Argon Laser (Coherent), tuned to 488 nm, and a 6 W Argon Laser (Spectra Physics), tuned to Multi-line-UV, were used. The two lasers are spatially resolved, so that no overlap between the respectively excited fluorescence signals will occur. Laser Output power was 100 mW for both lines. Filters used were a 530/30 BP filter for the Rh123 signal and a 424/44 BP filter for the DAPI signal. For sterile sorting the tubing of the cell sorter was decontaminated of remnants of previous samples and sterilised by running in succession as sheath fluid for 1 h each of the following solutions: 0.1N NaOH; 0.1% Triton X-100; 70% ethanol. Subsequently, a sterile sheath tank with PBS was connected to the cell sorter and the remaining ethanol rinsed out by running for 30 min.

Dead cells and cell debris were excluded based on absence of a DAPI fluorescence signal and on the forward scatter/side scatter signal (FSC-H/SSC-H). Sort gates on the viable cell population were set in a dot plot using FL1-H as y- and FSC-W as x-axis (Fig. 2). Cells with both top and bottom 3 % of fluorescence intensity were single cell sorted into the 96 well plates with the automatic cell deposition unit. The plates were prefilled with 100 μ l per well of a 1:1 mixture of cell culture medium as mentioned above and sterile-filtered culture supernatant to improve single cell cloning efficiency.

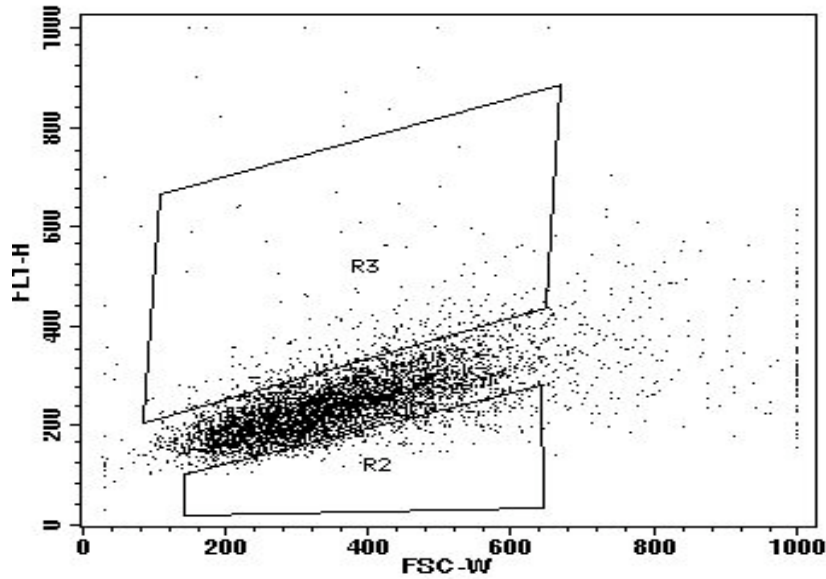


Fig. 2: Sort gates for cells with both low (R2) and high (R3) Rhodamine fluorescence.

After one week in the incubator, another 100 μ l per well of cell culture medium/culture supernatant mix was added to the sorted cells to boost growth of the cells. Another one to two weeks later the first subclones could be picked from the plates. The subclones were then carefully expanded to 24-well-, 12-well plates and small T-flasks (25 cm²) consecutively.

Quantitative hIgG ELISA

The product concentration was determined by ELISA (enzyme linked immunosorbent assay). A 96 well plate (NUNC maxisorp) was precoated with Anti-Human IgG (Sigma), able to catch the 2G12 antibody. The standard and the prediluted sample were added and the plate was washed after incubation. The bound antibody was then tagged with a polyclonal goat-anti-human IgG conjugated to horseradish peroxidase (HRP). After incubation and subsequent washing, the complex bearing the peroxidase was incubated with hydrogen peroxide and orthophenyldiamine (OPD), triggering a colour reaction, when two molecules of OPD condense. This reaction was stopped by addition of concentrated sulfuric acid after a well-defined period of time and evaluation was performed using an ELISA-reader. The concentrations were calculated according to standard curves.

Transcriptome analysis of sorted subclones

Isolation of total RNA

Total RNA of cell cultures was extracted on days 2 and 3 in the batch phase. Extraction was done using the Trizol reagent (Gibco, USA). 10^7 cells were harvested, spinned down for 10 minutes at 170 g, washed once with PBS and centrifuged again. Two ml of Trizol reagent were added to the cell pellet, mixed by pipetting up and down and put on the vortex for 10 seconds. Afterwards, the mixture was left to incubate at room temperature for 5 min, then it was stored at -80°C until purification of the RNA.

To each of the thawed Trizol samples (1 ml), 200 μl of chloroform were added. Mixtures were thoroughly vortexed, left to incubate at RT for 3 min and centrifuged at 14.000 g for 15 min. The lower, chloroform phase was then carefully removed, samples spun down again for 3 min and the upper aqueous phase transferred to a new tube. Then, 500 μl of isopropanol were added (1:2), carefully mixed by inverting the tube and incubated at RT for 10 min. The precipitate was spun down at 12.000 g for 10 min. The supernatant was removed and the pellet was washed once with ethanol (70 % [v/v]). After centrifugation of the pellet at 7.500 g for 5 min, the ethanol was removed and the pellet left to air-dry. It was then taken up in 50 μl of nuclease-free water and dissolved at 60°C for 10 min. All centrifugation steps were performed at 4°C . RNA content was determined by a spectrophotometer, concentrations lay between 1.000 and 2.500 $\mu\text{g}/\text{ml}$. RNA purity was determined by both measuring $A^{260/280}$ and on a bioanalyzer chip (Agilent, USA). Purified RNA samples were stored at -80°C .

Processing of isolated RNA

Isolated and purified total RNA from CHO cell cultures were processed according to the manufacturers manual for use on an Agilent oligonucleotide mouse 22K microarray (Agilent Technologies, USA). In short, cDNA was synthesised from isolated RNA, then transcribed into cRNA and purified. In this step, flurescently labelled nucleotides were incorporated into the resulting DNA. Afterwards, DNA was synthesised from cRNA for hybridisation.

For cDNA synthesis, 500 ng of total purified RNA were mixed with a T7 promotor primer, 5x First Strand Buffer, 0.1 M dithiothreitol (DTT), 10 mM dNTP mix, MMLV-reverse transcriptase and a RNase inhibitor (RNaseOUT) and incubated in a circulating waterbath at

40°C for 120 min. Subsequently, the mixtures were incubated at 65°C for 15 min for inactivation of the MMLV-RT and then put on ice for another 5 min.

cDNA was then transcribed to cRNA to incorporate cyanine dye-labelled nucleotides in a mixture with 4x Transcription Buffer, 0.1 M DTT, NTP and CTP mix, polyethylene glycol (PEG), RNaseOUT, inorganic pyrophosphatase and T7 RNA polymerase by incubation at 40°C for 120 min. cRNA was then purified on a column to remove unincorporated dye. Purity, concentration and success of incorporation of cyanine dyes was determined on a ND-1000 UV/VIS spectrophotometer (Nanodrop Technologies, USA). Each of the cDNA samples were transcribed using Cy3- and Cy5-labelled nucleotides separately to allow dye-swap experiments in the hybridisations for control reasons.

Using a similar protocol as for cDNA synthesis out of total RNA, fluorescent cDNA was then synthesised from cRNA and purified again.

Hybridisation, scanning and analysis of the cDNA microarrays

mRNA from both C2G12-LR2 and -HR1 were compared to the mRNA of the parental C2G12 cell line (C2G12-SFWCB) using five microarrays each. Four arrays were used for comparison, hybridising Cy5-labelled cDNA from either LR2 or HR1 together with Cy3-labelled cDNA from SFWCB (normal) on two arrays and swapping dyes on the other two. One array was hybridised with Cy3- and Cy5-labelled cDNA from either LR2 or HR1 (self-self experiment) for control reasons.

For the hybridisations, 750 ng of both cDNA to be compared were mixed, enzymatically fragmented and transferred to the arrays. Hybridisation took place on a rotating frame in an oven set to 60°C for 17 hours. Then, the arrays were washed, quickly dried with nitrogen and scanned on a DNA microarray scanner (Agilent, USA).

Data analysis was performed using GeneSpring software (Agilent, USA) and gene set enrichment analysis (GSEA) (Subramanian et al. 2005).

Results

Cell sorting

Figure 3 shows specific lactate production rates (qLac) of subclones retrieved from sorting experiments conducted earlier in this workgroup (Brugger 2005). Clones of the CHO cell line C2G12, that exhibited highest and lowest 3 % Rhodamine 123 fluorescent signal, were sorted into 96-well plates at one cell per well. From this sorting experiment, the subclone C2G12-LR2, being the one with the lowest value for qLac, was picked for further evaluation, as subject to the present work.

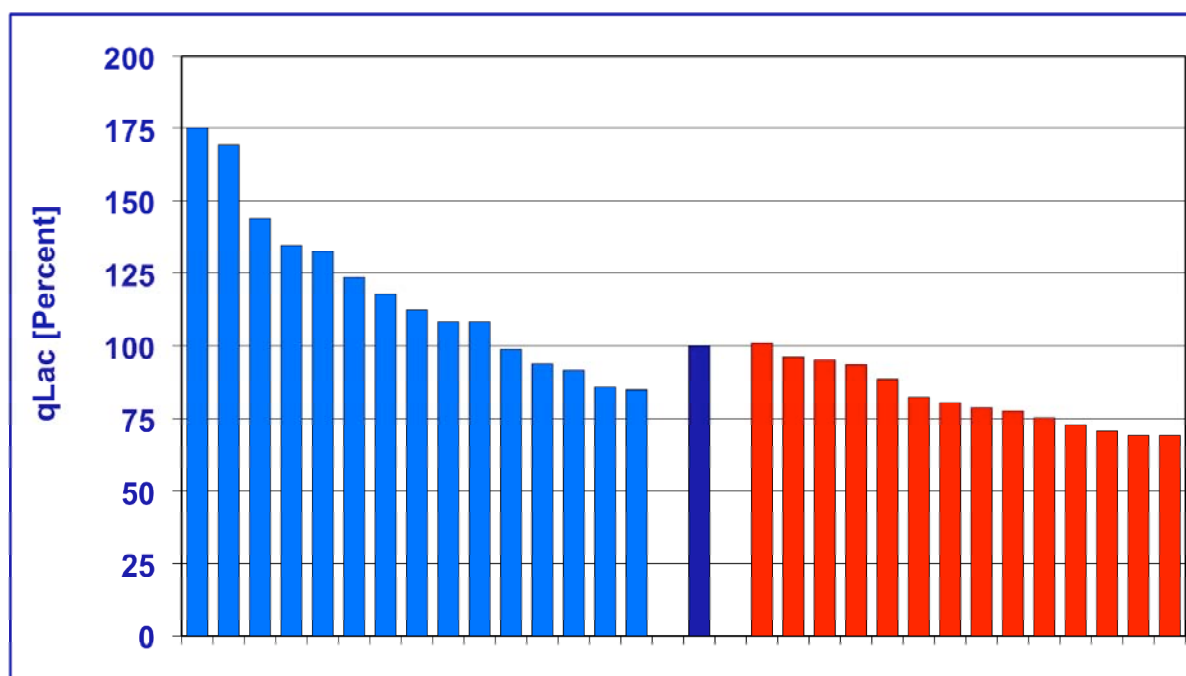


Fig. 3: Specific lactate production rates of C2G12 subclones sorted on low (red bars) and high (blue bars) Rhodamine 123 fluorescence in percent. The dark blue bar represents the corresponding value of the parental cell line as 100%.

Sorting experiments have been redone for the present work under the same conditions as for the experiment shown above. This time, specific lactate production rates for subclones sorted on both high and low Rhodamine 123 fluorescence showed a similar range and no improvement in comparison to the parental cell line could be observed (Fig. 4). The subclone C2G12-HR1, being the clone with the highest value for qLac among clones sorted on high Rhodamine 123 fluorescence, was picked from an earlier sorting experiment isolating only

subclones with high Rh123 signal, yielding only a small number of subclones (data not shown).

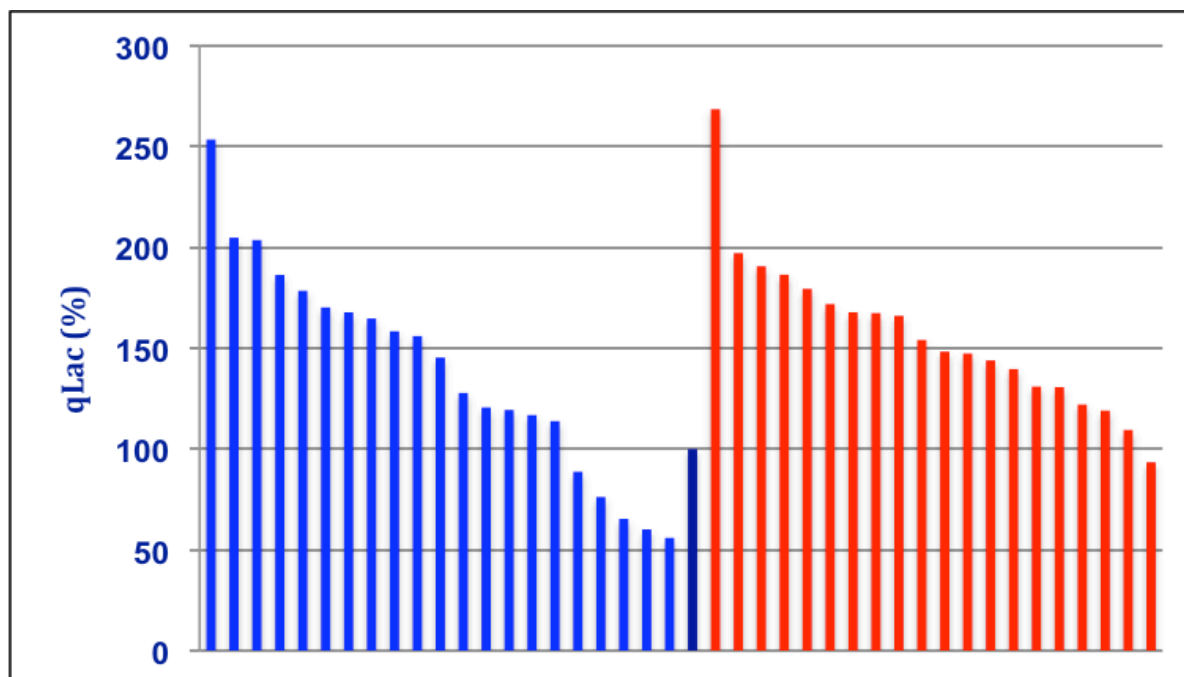


Fig. 4: Specific lactate uptake rates of sorted C2G12 subclones in percentage of the corresponding value of the parental cell line (dark blue bar). Blue bars indicate subclones with high and red bars subclones with low Rhodamine 123 fluorescence.

Batch cultures

The isolated subclone C2G12-LR2 was then further characterised in comparison to its parental cell line C2G12-SFWCB in a series of batch cultures in both roller bottles and spinner flasks. The subclone C2G12-HR1 was only characterised in batch cultures in spinner flasks.

Batch cultures in roller bottles

As mentioned before, batch cultures were started at an initial cell density of 2×10^5 viable cells per ml and at a culture volume of 200 ml.

Growth performance

The following graphs show viable cell concentrations for the parental C2G12-SFWCB and for the subclone LR2 (Fig. 5).

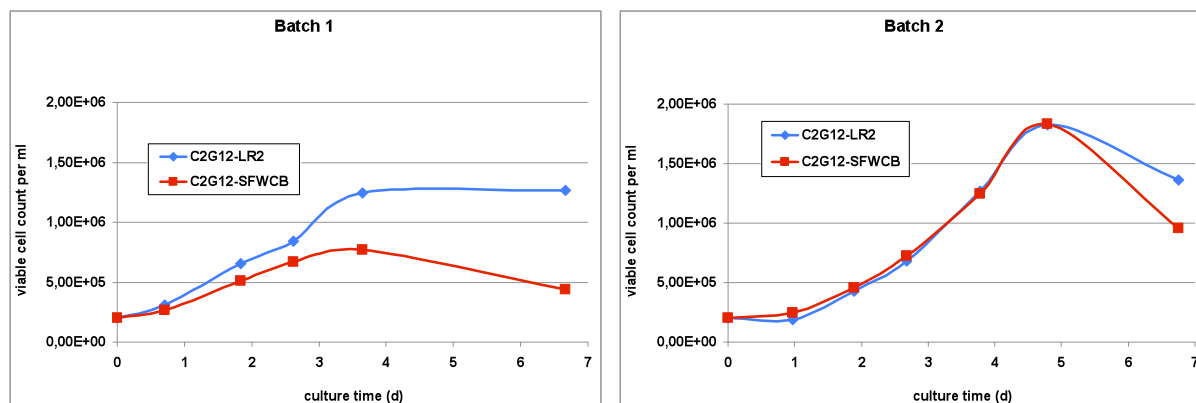


Fig. 5: Viable cell concentrations of C2G12-SFWCB (red graphs) and C2G12-LR2 (blue graphs) in cells/ml.

The final cell concentrations that were reached in both batches are low compared to other host and production CHO cell lines, which is due to the tetraploid character of the C2G12 cell line. In batch 1, the growth curve of the LR2 subclone significantly exceeds the one of the parental clone, which confirms earlier findings on this subclone. In batch 2, both subclones exhibit a similar growth performance. Subclone LR2 might have reached a higher end cell concentration in batch 1, since no sample has been drawn on day 5, like in batch 2. It should be emphasised that the growth performance of the parental clone is substantially elevated in comparison to normal cultivation behaviour.

Glucose uptake rates

Below, specific glucose uptake rates of C2G12-SFWCB and -LR2 of two individual batch cultures in roller bottles are shown (Fig. 6)

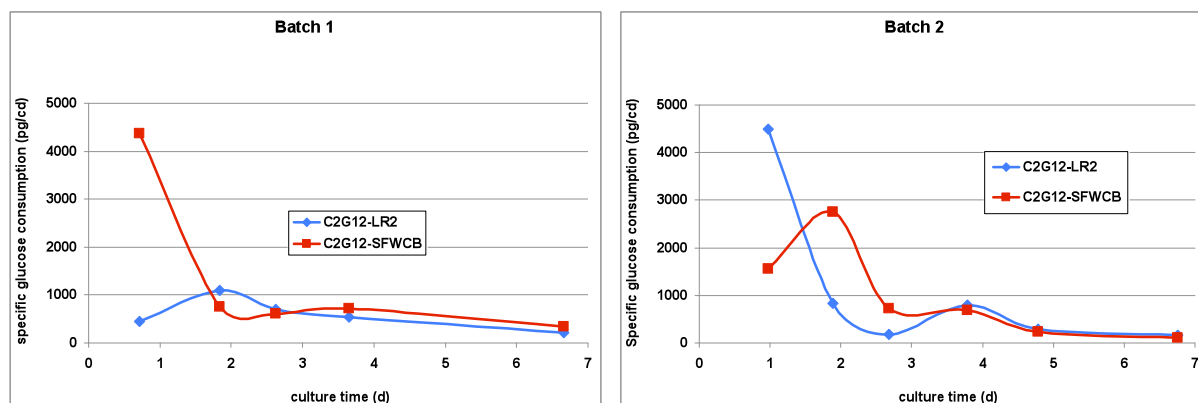


Fig. 6: Specific glucose consumption rates of C2G12-SFWCB (red graphs) and C2G12-LR2 (blue graphs) in pg/cd.

Figure 6 indicates a slightly elevated glucose consumption of the cell line C2G12-SFWCB when compared to -LR2. High variations of qGlc values are due to recurrent technical problems and day-to-day fluctuations when measuring glucose, lactate and glutamine with the YSI Multiparameter system. Glucose consumption rates were also calculated over the first 4 days of the batch culture, resulting in 700 and 810 pg/cd for C2G12-LR2 for batches 1 and 2 respectively, compared to 1030 and 890 pg/cd for C2G12-SFWCB.

Lactate production rates

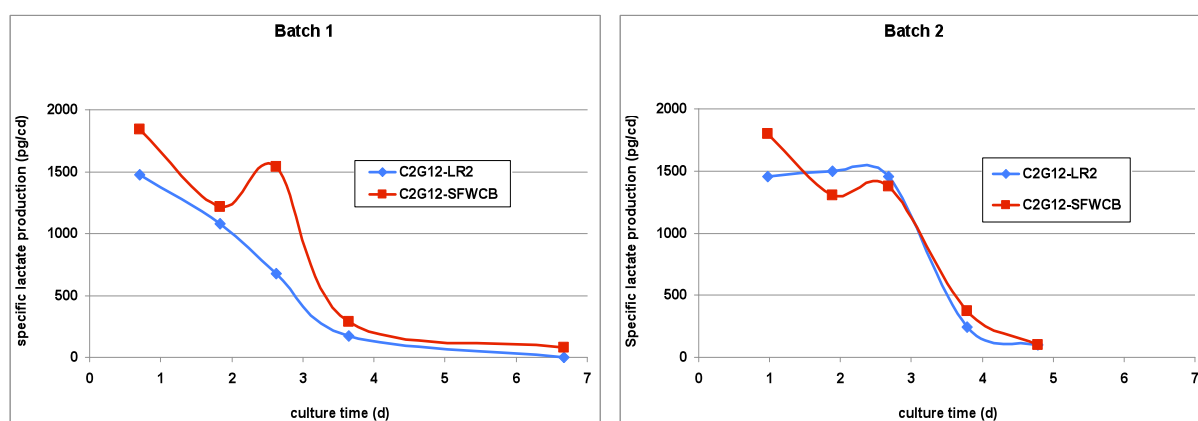


Fig. 7: Specific lactate production rates of C2G12-SFWCB (red graphs) and C2G12-LR2 (blue graphs) in pg/cd.

The lactate production rate of the LR2 subclone was significantly reduced in comparison to the parental clone in batch 1. The differences in metabolism appeared more clearly than in the

cell's glucose consumption. However, no differences in qLac values between the cell lines could be found in the second batch (Fig. 7). Again, as could be seen in the growth curves and qGlc values, SFWCB and LR2 exhibited similar performances in batch 2.

In batch 1, qLac:qGlc ratios, which indicate how much of the glucose has been converted to lactate, remain above 1 on the first 4 days of the batch. In batch 2, the ratio remains below 1 for the first 3 days in culture.

Glutamine uptake rates

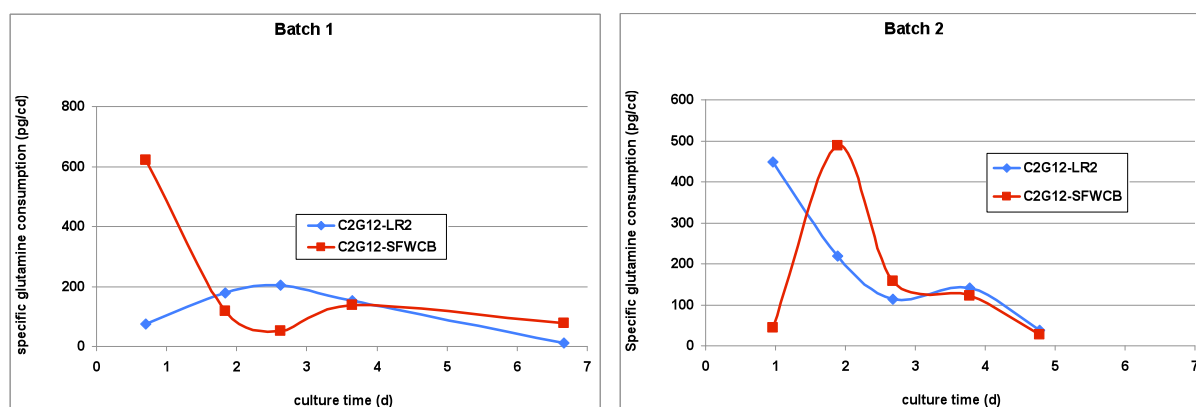


Fig. 8: Specific glutamine uptake rates of C2G12-SFWCB (red graphs) and C2G12-LR2 (blue graphs) in pg/cd.

Values for glutamine consumption fluctuated as well, exhibiting a tendency of slightly elevated qGln rates of the parental cell line, when compared to LR2 (Fig. 8).

Specific mAb productivity

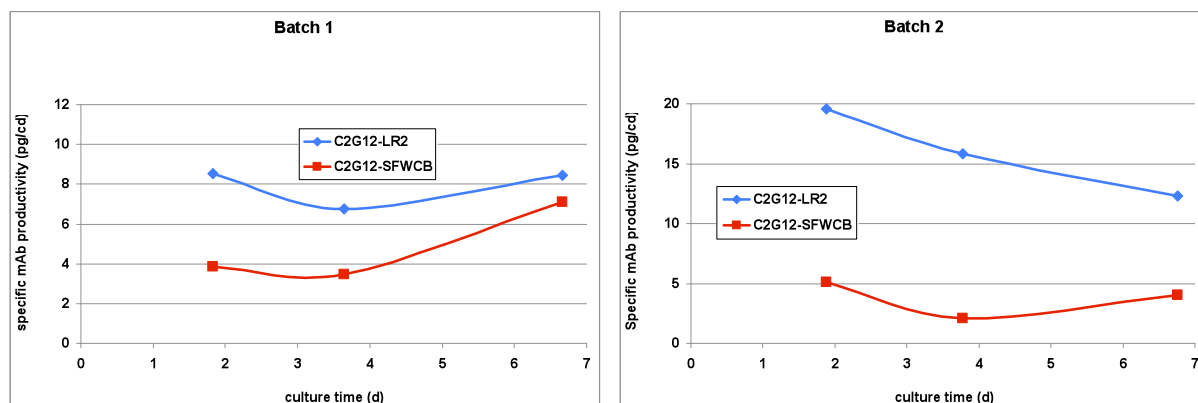


Fig. 9: Specific mAb productivity of C2G12-SFWCB (red graphs) and C2G12-LR2 (blue graphs) in pg/cd.

In both batch cultures, the subclone LR2 shows significantly higher specific antibody productivity than the parental cell line SFWCB (Fig. 9). The final product titer remains about the same for C2G12-SFWCB at 14.6 and 19 $\mu\text{g}/\text{ml}$ for the first and second batch respectively. C2G12-LR2 yields 49 and 60 $\mu\text{g}/\text{ml}$ in the two batches.

Summary

Important benchmark data of the two batches in the roller bottles are summarised in tables 1 and 2.

	viable cumulative celldays	\emptyset qGlc	\emptyset qLac	\emptyset qGln	\emptyset qP	final product titer ($\mu\text{g}/\text{ml}$)
LR2	6.12 e06	697	600	165	8.0	49.0
SFWCB	3.57 e06	1029	1001	156	5.4	19.1

Table 1: Performance summary of C2G12-SFWCB and -LR2 in the first batch cultivated in roller bottles.

	viable cumulative celldays	\emptyset qGlc	\emptyset qLac	\emptyset qGln	\emptyset qP	final product titer ($\mu\text{g/ml}$)
LR2	6.60 e06	1030	808	176	9.2	60.4
SFWCB	6.24 e06	1100	890	178	2.3	14.6

Table 2: Performance summary of C2G12-SFWCB and -LR2 in the second batch cultivated in roller bottles.

The C2G12-LR2 showed comparable growth in both roller batches. However, values for qGlc and qLac increased by 40 and 30% in the second batch, respectively. The specific productivity exceeded the one of SFWCB, especially in the second batch, which led to 2.5- and 4-fold increase in final antibody titer when compared to the parental cell line.

The C2G12-SFWCB on the other hand exhibited constant metabolic rates in both batches. In batch 2, the viable cumulative cell integral increased by a factor of 1.75 in comparison to batch 1. It remains unclear, whether the strong growth performance happened at the expense of specific mAb productivity, which decreased more than two-fold, or if then again declined mAb production facilitated better growth.

Batch cultures in spinner flasks

Metabolic and growth performances of C2G12-SFWCB, -LR2 and -HR1 were analysed and compared in 125 ml spinner flasks. Additionally, stability of metabolic characteristics of subclone LR2 was analysed in batch 1. Therefore, in this batch this subclone was run at 7th and 42nd passage, respectively. The C2G12-LR2 subclone in 7th passage was kept in cultivation and used for the second batch.

Transfer of the cells from T-flasks and roller bottles to a stirred cultivation system like spinner flasks, implied an increase in shear stress and a very long adaptation phase was necessary.

As described for the batch cultures in roller bottles, batches in spinner flasks were started at an initial viable cell count of 2×10^5 cells /ml and a starting volume of 100 ml.

Growth performance

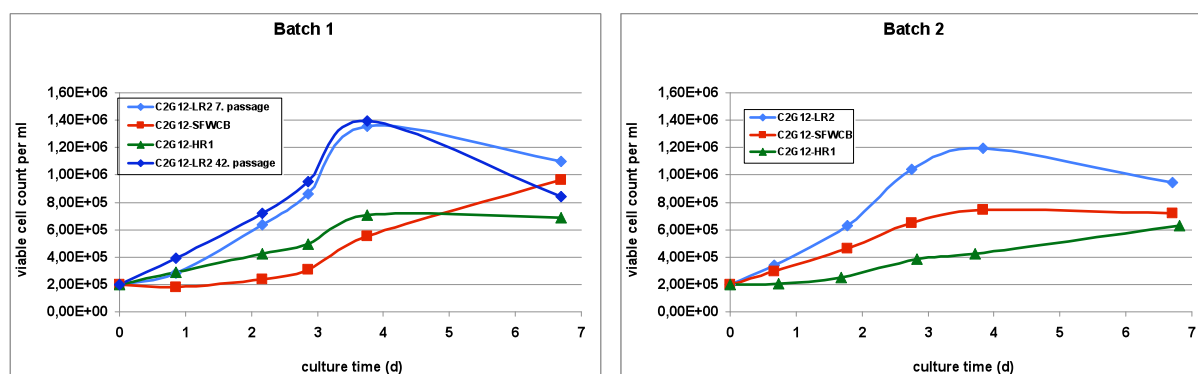


Fig. 10: Viable cell counts of C2G12-LR2 in 7. passage (light blue line), LR2 in 42. passage (dark blue line), SFWCB (red line) and HR1 (green line).

Cell concentrations for the subclone LR2 appeared constantly higher than the other clones over the whole batch phase in both cultivation experiments. The parental cell line showed a severe lag phase in batch 1, which allowed subclone HR1 to outperform the SFWCB until day 5. In the first batch, all three cell lines were still struggling to adapt to the spinner flasks, exhibiting viabilities between 80 and 89%. Batch 2 clearly showed the differences of the two subclones in comparison to the parental cell line as far as their growth capabilities are concerned (Fig. 10).

Specific glucose uptake

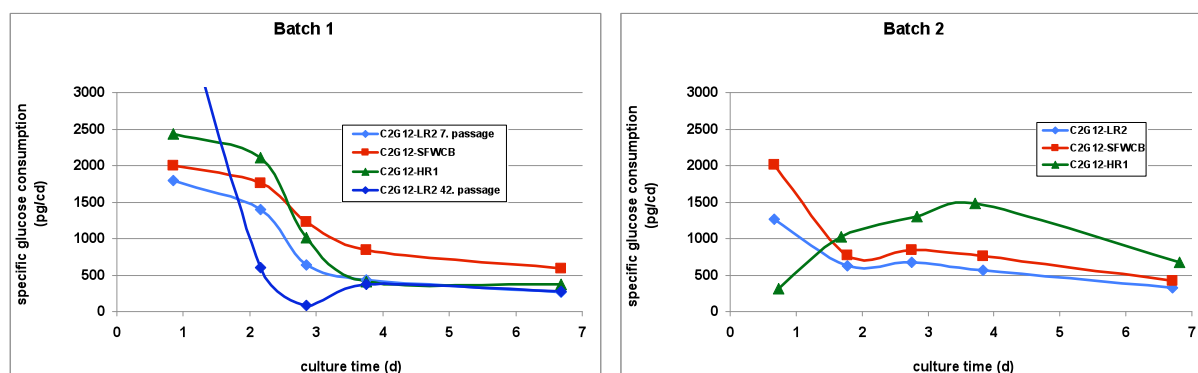


Fig. 11: Specific glucose uptake rates of C2G12-LR2 in 7. passage (light blue line), LR2 in 42. passage (dark blue line), SFWCB (red line) and HR1 (green line).

Again, the LR2 subclone showed the lowest qGlc values throughout both batch experiments, apart from the value for day one for the LR2 in 42nd passage, which was probably due to measurement errors of the YSI Multiparameter system. Glucose uptake rates of the subclone HR1 and the parental clone SFWCB exhibited no distinct differences in the first batch. The reason for that was plausibly the extended lag phase of the SFWCB as can be seen in the growth curve. In the second batch, all three cell lines conserved constant differences in their qGlc values over the batch phase (Fig. 11).

Specific lactate production

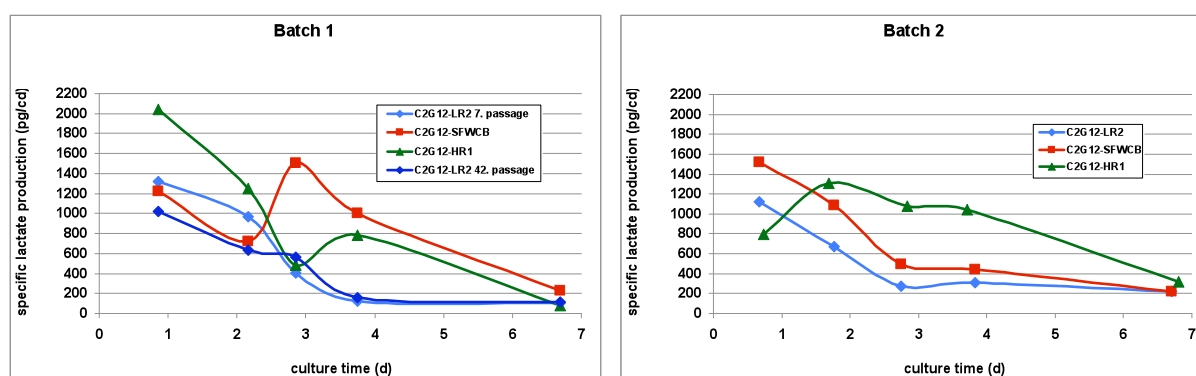


Fig. 12: Specific lactic acid formation rates of C2G12-LR2 in 7. passage (light blue line), LR2 in 42. passage (dark blue line), SFWCB (red line) and HR1 (green line).

LR2 exhibited the lowest qLac rates in both batches. The parental cell line again showed unusual high lactic acid formation beginning from day 3. Specific lactate production rates in the second batch confirmed the results for glucose uptake. All three cell lines showed values that constantly differed from each other over the whole batch phase (Fig. 12). The close relation between glucose uptake and lactate production can be seen in the comparison of both figures.

Specific glutamine uptake

Figure 13 shows specific glutamine consumption rates for all three subclones. No distinct differences between the subclones in glutamine metabolism could be observed.

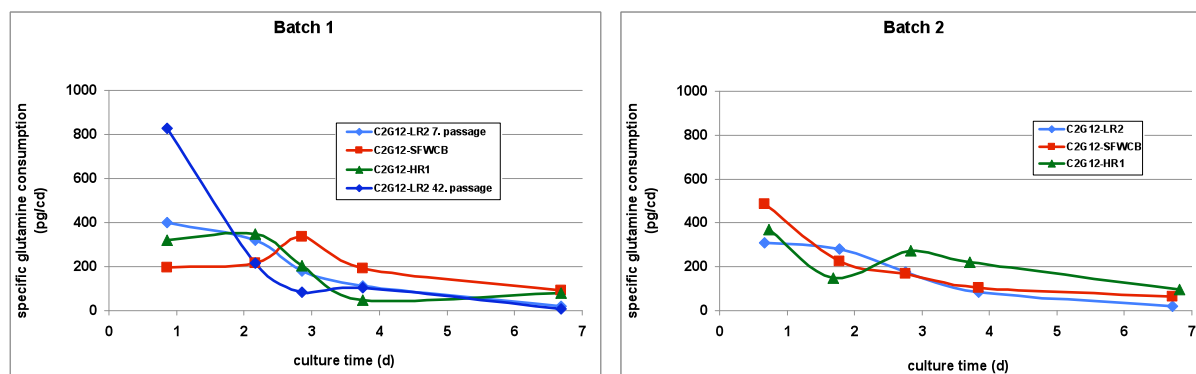


Fig. 13: Specific glutamine uptake rates of C2G12-LR2 in 7. passage (light blue line), LR2 in 42. passage (dark blue line), SFWCB (red line) and HR1 (green line).

Specific mAb productivity

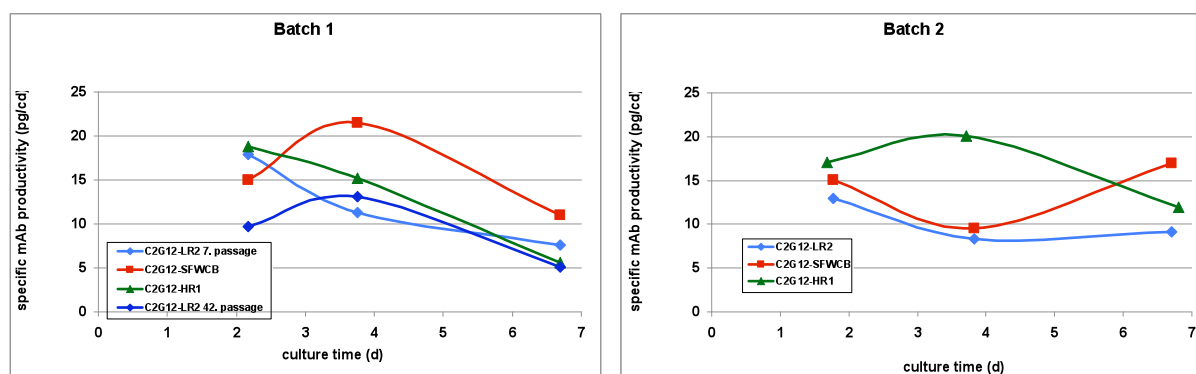


Fig. 14: Specific antibody productivity of C2G12-LR2 in 7. passage (light blue line), LR2 in 42. passage (dark blue line), SFWCB (red line) and HR1 (green line).

In spinner flasks, C2G12-LR2 had the lowest specific productivity of all three subclones, which remained the same irrespective of the age of the subclone. Interestingly, the parental cell line SFWCB reached higher productivity in the first batch, where the cell line obviously had problems with growth. Productivity of the SFWCB reached top level on day 4, together with its highest growth rate in the batch phase. MAb productivity of the subclone HR1 was consistent with LR2 in the first batch, but exceeded both other subclones in the second batch (Fig. 14).

Rhodamine 123 fluorescence

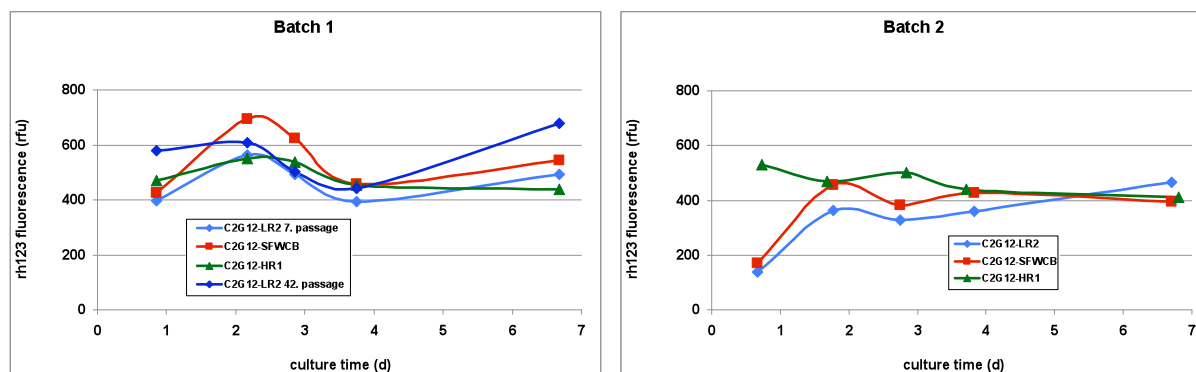


Fig. 15: Relative Rhodamine 123 fluorescence values of C2G12-LR2 in 7. passage (light blue line), LR2 in 42. passage (dark blue line), SFWCB (red line) and HR1 (green line).

In both batches, no distinct differences in Rhodamine 123 fluorescence values for all three subclones could be observed. In batch 2, fluorescence values differed slightly but not significantly in the first three days of the batch experiment. Increase of fluorescences in the first two days of the batches could be observed (Fig. 15). However fluorescence values for Rhodamine 123 remain more or less constant over the whole batch phase, which is not consistent with decreasing nutrient uptake and lactate production rates.

Summary

In tables 3 and 4, results from batch experiments with C2G12-LR2 in 7th and 42nd passage, -SFWCB and -HR1, are summarised. Values are calculated over the whole batch period.

	viable cumulative celldays	Ø qGlc (pg/cd)	Ø qLac (pg/cd)	Ø qGln (pg/cd)	Ø qP (pg/cd)	final titer (µg/ml)
LR2 7.P	5.85 e06	845	507	205	8.3	48.6
LR2 42.P	5.78 e06	777	463	199	6.4	37.0
SFWCB	3.17 e06	1356	1055	227	11.4	36.1
HR1	3.56 e06	1326	1032	209	7.9	28.2

Table 3: Summary of spinner batch 1.

	viable cumulative celldays	Ø qGlc (pg/cd)	Ø qLac (pg/cd)	Ø qGln (pg/cd)	Ø qP (pg/cd)	final titer (µg/ml)
LR2	5.76 e06	656	418	164	4.9	28.0
SFWCB	3.97 e06	896	695	183	9.0	35.6
HR1	2.69 e06	1168	1075	243	7.2	19.3

Table 4: Summary of spinner batch 2.

The C2G12-LR2 showed a consistent performance. The values for viable cumulative celldays and all rates related to the energy metabolism remained constant in both batches and regardless of the age of the culture. Specific productivity, however, appeared to decrease with age of the culture, leading to a lower final antibody titer than for the parental cell line in the second batch.

C2G12-SFWCB showed a severe distortion in growth and metabolism in the first batch. A very long lag phase led to a decrease in viable cumulative celldays and increased metabolic rates. Its specific productivity was higher than the ones of the two subclones. Regardless of the bad performance in the first experiment, final product titers were constant for both batch cultures.

The C2G12-HR1 exhibited a comparable metabolic performance in batch 1 and 2. Faster growth in the beginning of the first batch led to a higher viable cell integral, but metabolic rates and production rates are similar in both batches. The C2G12-HR1 yields less final antibody titer compared to the other cell lines due to its weak growth performance.

Transcriptional analysis

Analysis of self-self experiments for both subclones should help setting a threshold for fold change in gene expression. The fold change thresholds were set to values that were exceeded or underscored by only 0.5% of the genes in the self-self experiments. Genes with fold changes above 1.3 and beyond 0.7 were identified as regulated and included in the analysis. For the subclone LR2, 405 genes were found up- and 64 genes downregulated, for HR1, 307 genes were up- and 125 genes were downregulated, with p-values below 0.01.

For further analysis, a GSEA-add-on to Microsoft Excel was used. The gene sets that were used resembled those defined by the Kyoto Encyclopedia of Genes and Genomes (KEGG) as mentioned in the introduction. Therefore, the analysis part is split into four sections, dealing with the KEGG categories metabolism, genetic information processing, environmental information processing and cellular processes.

Since both C2G12 subclones LR2 and HR1 exhibited opposite growth and metabolic characteristics compared to the SFWCB, gene sets that are upregulated in the one subclone and downregulated in the other would be particularly interesting. Unfortunately, very few gene sets were regulated that way. Most regulations were found to be unilateral, showing difference to the reference SFWCB only for one subclone. All given transcriptional regulations in the next sections, if not stated otherwise, are of course always in comparison to SFWCB as reference.

Metabolism

The section Metabolism contains the most regulated gene sets by far. 12 gene sets were found to be regulated, three of them differentially for HR1 and LR2, the rest were regulated for one subclone only.

Glycerophospholipid metabolism:

This subset of genes describes the anabolic and katabolic metabolism of glycerophospholipids around the key elements 1,2-diacyl-sn-glycerol-3-phosphate, phosphatidylethanolamine and phosphatidylcholine (lecithin) (part of the pathway in Fig. 16). Conversion of phosphatidyl-L-serine to phosphatidylethanolamine is catalysed by the enzyme phosphatidylserine decarboxylase (*psid*), the reverse reaction by phosphatidylserine synthase (*ptdss*). The first one appears to be strongly upregulated in LR2 with no change in HR1, the latter is reduced in LR2 and slightly elevated in HR1. Additionally, HR1 shows a severe decrease of mRNA for the enzyme ethanolamine-phosphate cytidyltransferase, which activates phosphoethanolamine by addition of a cytidyl residue (CDP), which is then converted to phosphatidylethanolamine. Subclone LR2 shows highly elevated transcription in a pre-stage of building 1,2-diacyl-sn-glycerol-3-phosphate. Reactions catalysed by upregulated enzymes are marked with bold arrows in all pathway figures below.

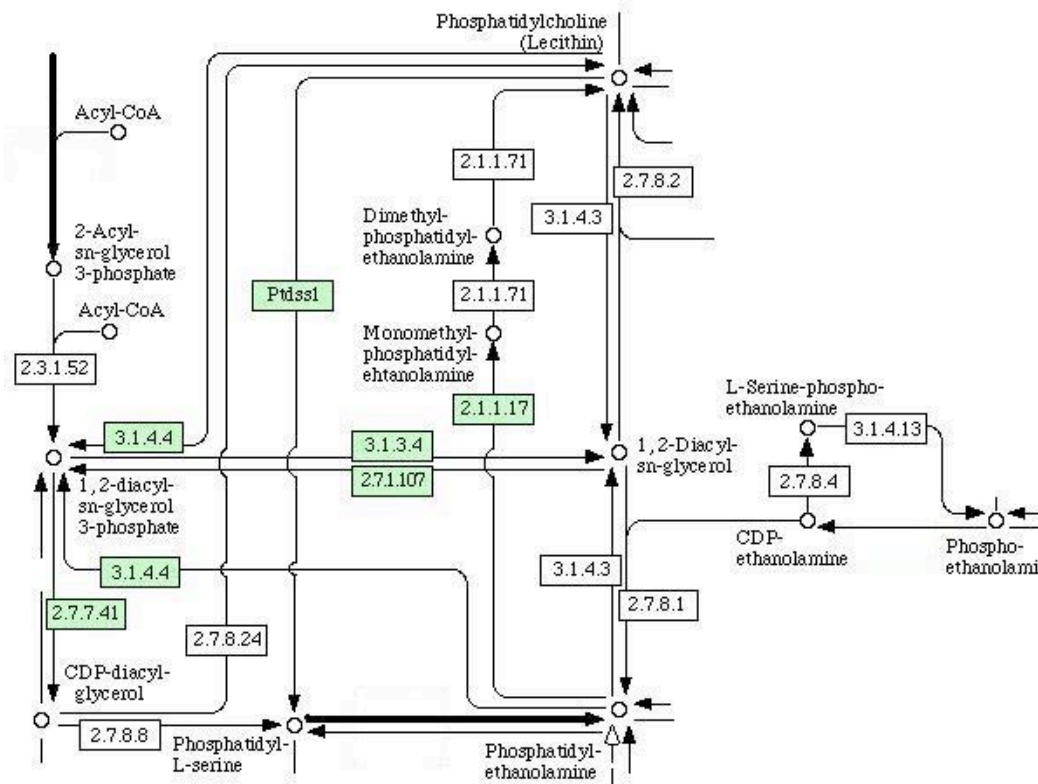


Fig. 16: Partial pathway glycerophospholipid metabolism from KEGG.

Oxidative Phosphorylation:

The pathway oxidative phosphorylation, which comprises all genes of the mitochondrial respiratory chain, appears to be downregulated in LR2 and upregulated in HR1. Decreased mRNA contents of certain subunits of the enzyme cytochrome c oxidase in LR2 (and vice versa elevated in HR1) can be held responsible for that. Also, all but one (Ndufa13) subunits of the gene for NADH dehydrogenase reach significantly higher transcription levels in HR1.

Synthesis and degradation of ketone bodies & Steroid biosynthesis:

The KEGG pathway synthesis and degradation of ketone bodies is structured around acetoacetyl-CoA as key factor and both its condensation with acetyl-CoA from glycolysis and lysis of the resulting product, setting free acetyl-CoA again. Steroid biosynthesis comprises the mevalonate (starting with 3-hydroxy-3-methylglutaryl-CoA) and the non-mevalonate pathway (starting from glyceraldehyde-3-phosphate) pathway, both resulting in isopentenyl-

pyrophosphate as the center point. After conversion to farnesyl-PP, the pathway is split into biosynthesis of vitamin E, cholesterol and precursors of phytosterols.

A close relation between these two pathways came up during microarray analysis. Whereas HR1 was left unaffected, LR2 exhibited an upregulation of the gene 3-hydroxy-3-methylglutaryl-Coenzyme A synthase with simultaneous decrease of 3-hydroxy-3-methylglutaryl-Coenzyme A lyase. Acetoacetyl-CoA is converted into the intermediate (S)-3-hydroxy-3-methylglutaryl-CoA, an entering point to steroid biosynthesis, which seems to be accumulated, since reaction to acetoacetate catalysed by the lyase mentioned above is decreased (Fig. 17).

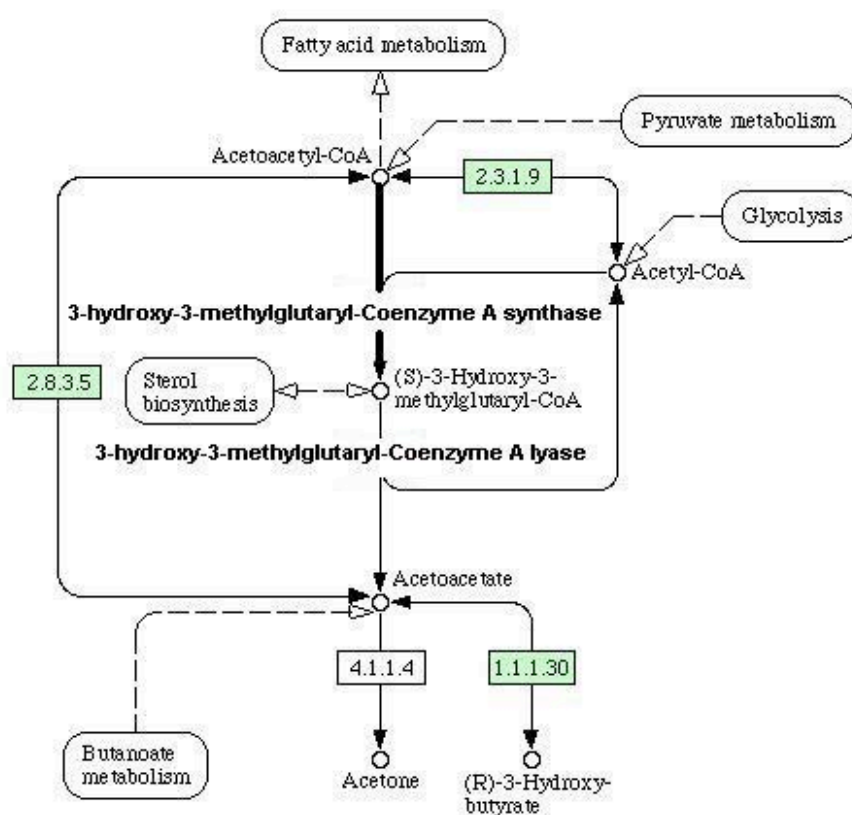


Fig. 17: Gene set synthesis and degradation of ketone bodies from KEGG.

(S)-3-hydroxy-3-methylglutaryl-CoA is the starting point for the mevalonate pathway (Fig. 18) of KEGG category *steroid biosynthesis*, which as a whole is also indicated as upregulated by gene set enrichment analysis. Especially genes that are responsible for the turnover of (S)-3-hydroxy-3-methylglutaryl-CoA into mevalonate and isopentenyl-PP into farnesyl-PP

(directly or via dimethylallyl-PP and geranyl-PP), reach distinctly higher mRNA copy numbers in LR2 than in SFWCB .

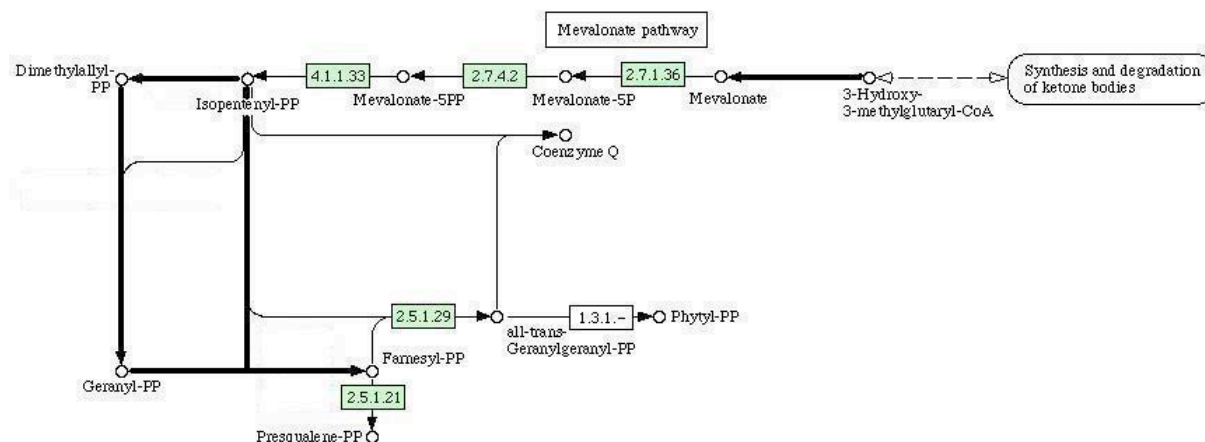


Fig. 18: Mevalonate pathway of KEGG subset *steroid biosynthesis*.

Farnesyl-PP is substrate to synthesis of e. g. carotenoids, cholesterol and phytosterols. LR2 shows elevated mRNA levels for some more genes along sterol biosynthesis and a specific and significant downregulation of the gene squalene epoxidase that produces (S)-squalene-2,3-epoxide. From this point on, sterol biosynthesis is split into three pathways, which are synthesis of either cholesterol, stigmasterol or vitamin E.

Spingolipid metabolism:

Spingolipids are important parts of lipid bilayer membranes in the cell. This KEGG pathway deals with synthesis and degradation of spingolipids around the two main elements *sphingosine* and *ceramide* (Fig. 19).

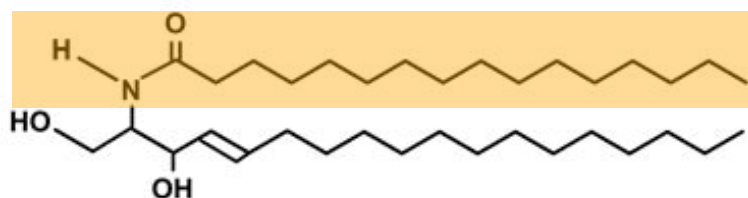


Fig. 19: Ceramide. The part highlighted orange is sphingosine.

The whole gene set seems to be elevated in LR2, which two distinct, highly upregulated genes can be held accountable for. The first one, *acidic glucosidase beta*, is responsible for turnover of glucosyl-ceramide, that results from degradation of glycosphingolipids, into ceramide. The second one, *N-acylsphingosine amidohydrolase*, splits the fatty acid off of ceramide, leaving sphingosine.

Genetic information processing

Both LR2 and HR1 seem to have a slight deficit in ribosomal activity compared to the reference clone SFWCB. The KEGG pathway *ribosome*, which mainly consists of genes of ribosomal subunits, is significantly downregulated in both subclones.

Environmental Information Processing

Gene sets in this KEGG pathway are involved in cell-cell or cell-ECM communication and interaction in fields like *Notch*, *phosphatidylinositol* and *Wnt signalling pathways*, as well as *ECM-receptor interaction* and *ion-coupled transmembrane transport*. Some of these pathways appear to be differentially regulated in the C2G12 subclones in comparison to the parental cell line. Wnt- and phosphatidylinositol signal pathways are slightly elevated in HR1 and decreased in LR2, Notch signalling and ECM-receptor interaction are elevated in LR2 and decreased in HR1. Due to difficulties in understanding the mode of action of these pathways in an immortalised single cell suspension culture, obtained expression data is left out of the present work.

Cellular Processes

All other pathways and processes inside the cell are allocated to the KEGG category *Cellular Processes*. It contains a wide variety of subsets, that partly can again not be interpreted since the cells remained no longer in their original tissue environment. The gene set *cell cycle* exhibits a negative score for both the HR1 and the LR2 subclone, which is surprising bearing in mind the LR2's improved growth characteristics. However, there are differences in expression the genes are scanned one by one.

Discussion

Immortalised mammalian cell lines lack the ability to efficiently metabolise glucose to CO₂ and water. Most of the glucose enters the glycolytic pathway, but instead of being transferred into the mitochondria and into the citric acid cycle, the resulting pyruvate is converted to lactate. This conversion discharges only a fraction of the energy, that could be achieved in the citric acid cycle. Therefore, glutamine has to be substituted, which can nearly completely enter the citric acid cycle and ensures energy supply for the cells. Metabolism of glutamine in the cell causes release of ammonia into the cytoplasm and the mitochondrial matrix, which interferes with the glycosylation machinery in general and terminal sialylation in particular (Grammatikos et al. 1998, Valley et al. 1999). Reduction and/or change in sialylation patterns would have a drastic impact on the effect and retention of these products in the human body.

The ideal immortalised mammalian cell would act as if it was still part of its original tissue and completely oxidise and derive most of the energy it needs from glucose, which would make supplementation of glutamine dispensable. Growth inhibitory or toxic effects of the formation of lactate and ammonia would be largely reduced, allowing longer cultivation periods, higher cell counts and therefore higher product yields. Due to the complexity and integration of the mammalian energy metabolism, the feasibility of engineering an ideal cell is unlikely. However, many attempts have been made to achieve some improvement in this field, using diverse approaches.

The present work makes use of a certain heterogeneity in metabolic characteristics within a cell population. Due to mechanisms such as transcriptional and translational regulation, epigenetic gene silencing, or minor mutations, the energy metabolism and therefore values of nutrient uptake and waste product secretion can differ largely from cell to cell. This fact can be exploited for development of cell lines with an improved metabolism, i. e. a more efficient utilisation of glucose.

(Borth et al. 1993) have shown a correlation between the intensity of the mitochondrial membrane potential (MMP) and the cell's actual glucose uptake rate, which is again largely dependent on the glucose concentration in the medium. The lipophilic cationic dye Rhodamine 123 has repeatedly been used to measure the MMP of different cell lines, making use of quenching of the Rh123 fluorescence in proximity of electrostatically charged

environments (Chen 1989, Baracca et al. 2003, Salvioli et al. 1997, Johnson et al. 1981). Fluorescence activated cell sorting (FACS) allows to isolate single cells with the desired metabolic characteristics. Additionally, transcriptional and/or translational analysis (genomics and proteomics) of isolated, improved subclones, could help elucidate responsible changes in the mechanisms of metabolism.

Antibody-producing CHO cell lines have been stained with Rhodamine 123 and sorted for both low and high Rh123 fluorescence and expanded. Glucose metabolism of retrieved subclones was analysed in short batch cultures, showing a strong tendency towards low qLac values for subclones sorted for low Rh123 signal and vice versa for subclones sorted for high Rh123 signal. The most promising candidate subclone (C2G12-LR2) was analysed further. A subclone sorted for high Rh123 fluorescence was analysed as well (C2G12-HR1). However, a second sorting experiment for both low and high Rh123 fluorescence did not succeed, with collected values for qLac being equally distributed for both low Rh123- and high Rh123-subclones. An explanation could be a certain non-coherence of the Rhodamine 123 signal to the cell's metabolic status, since the mitochondrial membrane potential reacts to other events in the cell as well. For instance, an early sign of apoptosis is the elevation of the MMP, which might corrupt the Rh123 fluorescent signal. Repeated bulk sorting of cells with a low Rh123 signal could help in getting rid of cells with unspecific Rh123 fluorescence and enrich cells with constant signals. Furthermore, an artificial increase of the cells' glucose uptake rate, e. g. by elevating the glucose concentration in the medium before the sorting experiment or by sorting at an early timepoint in culture, could lead to a better resolution of differences in metabolism between cells.

The metabolic characteristics of the subclones C2G12-LR2 and -HR1 were analysed by a series of batch cultures in comparison to the parental cell line C2G12-SFWCB (serum-free working cell bank). The cultivation experiments were carried out in two different types of culture vessels, roller bottles and spinner flasks. Heavy formation of cell aggregates in the roller bottles, especially at the end of the batch cultures, was the reason to switch to stirred culture vessels to redo the experiments. Due to their sensitivity to shear stress, adaptation of the C2G12 subclones to spinner flasks required lots of time and patience. Problems were finally resolved with addition of an anti-clumping agent (Gibco, USA), which decreased cell aggregation.

Batch experiments in the roller bottles showed highly different performances for the parental cell line. In contrast to the first batch, where a significant distinction not only in growth speed and final cell concentration, but also in specific metabolic rates is clearly visible, the SFWCB exhibited a performance, that was virtually identical to the one of LR2 in the second batch. The viable end cell concentration in batch 2 was high for both clones compared to earlier findings. In case of the SFWCB, the growth speed appeared to happen at the expense of specific productivity, which decreased from batch 1 to batch 2. The LR2 had a higher productivity and kept it stable in both batches, which led to a substantially higher antibody yield than for the SFWCB. The reason for this significantly altered growth of the SFWCB is likely just a natural variation in performance of mammalian cell lines, which is partly due to cell age, pre-cultivation of the cells, transfer of the cells while they are still in an exponential growth phase, starting conditions and more. Both cultures were started sequentially out of the same culture with a time-lag of six weeks, which equals about 12 passages. However, it could be shown in the spinner experiments, that these characteristics were stable for over 40 passages, enduring even intermittent drops of viabilities to around 60% in the process of adaptation to the spinner flasks.

In both batch cultures in spinner flasks, the subclone C2G12-HR1, sorted for high Rh123 fluorescence, and in the first batch, two cultures of different age of the LR2 (7th and 42nd passage) were included in the experiments. The subclone LR2 showed consistently improved growth characteristics and metabolic rates. The viable cell integral increased about 50%, overall glucose uptake decreased by at least 30%, and lactate production rates by at least 40% in comparison to the parental cell line. Consumption of glutamine showed no significant change. The age of the culture appeared to have an impact on specific productivity of the LR2 subclone, as batch experiments started out of cultures in the 42nd passage exhibited a slight decrease in specific antibody production. The younger culture was continued for another 12 passages and used for the second spinner batch experiment, showing strong decrease in productivity. The parental cell line had troubles growing in the first batch. It was exceeded in growth and equalled in its metabolic rates by the subclone HR1, which had shown inferior performance in the whole preceding cultivation and spinner adaptation process. Values for qGlc and qLac are increased compared to the ones of the second batch and also to the batches in the roller bottles. However, specific productivity of the parental cell line heavily increased

in comparison to cultivation in roller bottles, leading to a final mAb titer higher than in the LR2 cultures. Together with the fact that viabilities were below 90% for the whole batch culture, this probably indicates an incomplete adaptation to the higher requirements on robustness in spinner flasks. Regarding growth and metabolism, the subclone HR1 exhibited opposite characteristics compared to LR2, apart from specific mAb productivity, which could be stably maintained in both batch experiments.

Rhodamine 123 fluorescence was also monitored daily in the spinner batch experiments. However, no differences in fluorescent signals could be found, that would resemble the differences of the clones regarding their metabolism. Signal intensities generally increased between days 1 and 2, which may have its reasons in the lag phase of cells at the beginning of a batch, where the cells adapt themselves to the new environment (fresh medium, lack of growth factors, changed pH and pO₂). After adaptation, they start to grow exponentially, take up more nutrients, thus elevating their MMP and therefore Rhodamine 123 fluorescence. Lack of a fluorescence decrease over the batch phase, resembling declining nutrient uptake rates, either implies a constant MMP during batch culture, or raises the question, to which degree Rh123 staining of CHO cells in culture is indeed sensitive for mitochondrial activity. However, it should be stated, that the obtained results are contradictory to earlier outcomes of similar experiments (Brugger 2005).

The switch from roller bottles to spinner flasks appeared to have an impact on both LR2 and SFWCB. First, both clones yielded a slightly smaller viable cell integral in the spinner flasks, which is likely a result of the this cell line's sensitivity to shear stress. More importantly, specific antibody productivity significantly increased for the parental cell line SFWCB. At first, LR2 exhibited no changes in productivity in the first spinner batch compared to cultivation in the roller bottles, but had troubles maintaining it with increasing age of the culture. However, it could be shown in both cultivation systems, that sorting for low Rhodamine 123 fluorescence yielded a subclone, that exhibited reduced consumption of glucose and formation of lactate combined with significantly accelerated growth. These properties remained stable for at least 24 weeks. Sorting for high Rh123 fluorescence on the other hand yielded a subclone (HR1) with the exact opposite metabolic behaviour as the low Rh123 subclone (LR2), given the parental cell line as reference. Glutamine consumption rates and the qLac:qGlc ratios of both the LR2 and HR1 subclone and the parental cell line

remained the same. Therefore, reduction of glutamine uptake and therefore a decreased release of ammonia into the cell could not be achieved. Unaltered qLac:qGlc ratios suggest a similar efficiency in glucose metabolism in both subclones and the SFWCB. However, the reduced glucose uptake and lactate production of the subclone LR2 apparently results in highly improved growth characteristics.

As explained in a previous section, the collected data from microarray analysis was interpreted on the basis of biological pathways according to the *Kyoto Encyclopedia of Genes and Genomes* (KEGG). Negative or positive scores were allocated according to the magnitude of up- and down-regulation of the individual genes of these pathways.

Korke et al. (2004) analysed transcriptional profiles of cells with a shifted metabolism, which revealed clear changes in expression of key glycolytic and other metabolism-related genes. In this case, however, transcriptional analysis of the two subclones in comparison to their parental cell line, did not give any “easy” or obvious explanations for their phenotypical metabolic characteristics. Also, it should be emphasised, that the present microarray experiments rely on only one batch experiment, thus probably explaining the existence of both “reasonable” and “unreasonable” results. More batch experiments and microarray analysis of more RNA samples from different time points during the batches should help exclude coincidental effects and reveal consistent changes in gene expression. The true biological repeat of this experiment would be of course the retrieval and transcriptional analysis of more improved subclones from different parental cell lines.

Unsurprisingly, most of the regulated pathways in both LR2 and HR1 were part of the KEGG category *metabolism*. However, key elements of the energy metabolism were generally left unaffected, with the exemption of oxidative phosphorylation. OxPhos appears to be downregulated in a subclone that takes up less glucose and produces less lactate (LR2) than its parental cell line. This somewhat contradicts the original assumption, that LR2 is capable of shuffling more glucose, or pyruvate, into the tricarboxylic acid cycle (TCC). This fact is even more interesting, as the subclone HR1 exhibits a slight upregulation of the OxPhos pathway. Microarray experiments show that differential expression of only cytochrome c oxidase and NADH dehydrogenase are responsible for regulation of the OxPhos pathway.

This leaves the question, how the LR2 subclone meets its energy requirements with unaltered glutamine consumption, reduced glucose uptake and obviously decreased respiratory activity. It seems as if this subclone is just more “frugal” than its parental cell line.

Strictly speaking, transcriptional analysis did not come up with any more information that can be directly related to explaining the oppositional metabolic phenotypes of the C2G12 subclones.

However, LR2 exhibited an increase of activity in parts of its lipid metabolism. It appears that more pyruvate from different sources is pumped into the mevalonate (or 3-hydroxy-3-methylglutaryl-CoA reductase) pathway than in the parental cell line. Several genes that are responsible for conversion of acetoacetyl-coenzyme A to 3-hydroxy-3-methylglutaryl-Coenzyme A (HMGCoA) and further to farnesyl-pyrophosphate and geranylgeranyl-PP (*mevalonate pathway*) are strongly upregulated. The mevalonate pathway is an important cellular metabolic pathway present in all higher eukaryotes and many bacteria. It is important for the production of dimethylallyl pyrophosphate (DMAPP) and isopentenyl pyrophosphate (IPP), which serve as the basis for the biosynthesis of molecules used in processes such as cell membrane maintenance, hormones and *N*-glycosylation (Swanson and Hohl 2006). It is also a part of steroid biosynthesis. Farnesyl-PP and Geranylgeranyl-PP are substrates for synthesis of – among others – carotenoids, cholesterol and phytosterols and are needed for prenylation of membrane-anchored proteins, which is the attachment of lipid chains to proteins to facilitate their interaction with the cell membrane. For LR2, upregulation of the mevalonate pathway first and foremost means availability of substrates as building blocks of membranes, which is needed due to the higher growth rate of the subclone. Intermediates of the mevalonate pathway are substrates for vitamins and hormones, that are crucial for the cell. Also, growth factor signalling largely depends on membrane anchored, prenylated G-proteins, which might add to the subclone’s improved growth characteristics.

Elevated transcription levels of several genes in one pathway leading to more product or outcome may not essentially cover the whole subject. Increase of enzyme expression may be due to abundance or deficiency of a specific substrate. Entry points of two pathways of the lipid metabolism that require acetyl-CoA as substrate are upregulated (glycerophospholipid metabolism and the mevalonate pathway) in LR2. However, deducing this fact to the origin of acetyl-CoA, the linkage between glycolysis and TCC, would be too speculative, given the small amount of transcriptional analysis data available.

Several pathways have been investigated in the other three KEGG categories (*genetic information processing*, *environmental information processing* and *cellular processes*), that were employed for the present transcriptional study. Although slight differential regulations of some of these pathways could be found in the C2G12 subclones in comparison to the parental clone, it is difficult, if not yet impossible to interpret information, which has been derived from an immortalised, single cell suspension culture, about pathways originally active in multicellular organisms.

Conclusion

Immortalised mammalian cell lines, though crucial for today's biotechnological industry, have a defect energy metabolism, that might undercut their essential virtues, such as proper glycosylation. In the present work, it could be shown, that these cell lines bear the possibility of an improvement of their metabolism, which likely has a positive effect on their growth characteristics as well. With a simple staining procedure and the help of fluorescence activated cell sorting (FACS), a subclone, that exhibited a significantly reduced nutrient uptake and waste production in combination with accelerated growth, could be isolated out of an established, stably antibody-producing cell line. These new properties were shown to be stable over a period of about 6 months. An attempt to elucidate the background of this effect on the transcriptional level employing microarray technology unfortunately left most of the questions open. It can be stated that the metabolic phenotype of the isolated subclone cannot be deduced from alterations in key pathways of the energy metabolism. However, a significant upregulation of a certain part of lipid metabolism (the mevalonate pathway), that among others provides substrates and building blocks for membranes, hormones, vitamins and protein lipidation, might contribute to the improved performance of the subclone. More analysis on this subclone and on others in the future might clear up the underlying transcriptional, translational and regulatory status of this improvement.

Due to its simplicity and noninvasive nature, this staining and sorting technique can be proposed as an improvement tool for mammalian cell lines, not only in the process of development, but also for already existing host and production cell lines.

Literature

- Altamirano, C., C. Paredes, J. Cairó & F. Gòdia (2000) Improvement of CHO cell culture medium formulation: simultaneous substitution of glucose and glutamine. *Biotechnol Prog*, 16, 69-75.
- Arden, N. & M. Betenbaugh (2004) Life and death in mammalian cell culture: strategies for apoptosis inhibition. *Trends Biotechnol*, 22, 174-80.
- Baracca, A., G. Sgarbi, G. Solaini & G. Lenaz (2003) Rhodamine 123 as a probe of mitochondrial membrane potential: evaluation of proton flux through F₀ during ATP synthesis. *Biochim Biophys Acta*, 1606, 137-46.
- Bollati-Fogolín, M., G. Forno, M. Nimtz, H. Conradt, M. Etcheverrigaray & R. Kratje (2005) Temperature reduction in cultures of hGM-CSF-expressing CHO cells: effect on productivity and product quality. *Biotechnol Prog*, 21, 17-21.
- Borth, N., G. Kral & H. Katinger (1993) Rhodamine 123 fluorescence of immortal hybridoma cell lines as a function of glucose concentration. *Cytometry*, 14, 70-3.
- Brugger, G. 2005. Analysis of Energy Metabolism in CHO Cells (diploma thesis).
- Chen, K., Q. Liu, L. Xie, P. Sharp & D. Wang (2001) Engineering of a mammalian cell line for reduction of lactate formation and high monoclonal antibody production. *Biotechnol Bioeng*, 72, 55-61.
- Chen, L. 1989. Fluorescent labeling of mitochondria. 103-123. *Methods in Cell Biology*.
- Ernst, W., E. Trummer, J. Mead, C. Bessant, H. Strelec, H. Katinger & F. Hesse (2006) Evaluation of a genomics platform for cross-species transcriptome analysis of recombinant CHO cells. *Biotechnol J*, 1, 639-50.

- Europa, A., A. Gambhir, P. Fu & W. Hu (2000) Multiple steady states with distinct cellular metabolism in continuous culture of mammalian cells. *Biotechnol Bioeng*, 67, 25-34.
- Grammatikos, S., U. Valley, M. Nimtz, H. Conradt & R. Wagner (1998) Intracellular UDP-N-acetylhexosamine pool affects N-glycan complexity: a mechanism of ammonium action on protein glycosylation. *Biotechnol Prog*, 14, 410-9.
- Johnson, L., M. Walsh, B. Bockus & L. Chen (1981) Monitoring of relative mitochondrial membrane potential in living cells by fluorescence microscopy. *J Cell Biol*, 88, 526-35.
- Kanehisa, M., M. Araki, S. Goto, M. Hattori, M. Hirakawa, M. Itoh, T. Katayama, S. Kawashima, S. Okuda, T. Tokimatsu & Y. Yamanishi (2008) KEGG for linking genomes to life and the environment. *Nucleic Acids Res*, 36, D480-4.
- Kanehisa, M. & S. Goto (2000) KEGG: kyoto encyclopedia of genes and genomes. *Nucleic Acids Res*, 28, 27-30.
- Kanehisa, M., S. Goto, M. Hattori, K. Aoki-Kinoshita, M. Itoh, S. Kawashima, T. Katayama, M. Araki & M. Hirakawa (2006) From genomics to chemical genomics: new developments in KEGG. *Nucleic Acids Res*, 34, D354-7.
- Keij, J., C. Bell-Prince & J. Steinkamp (2000) Staining of mitochondrial membranes with 10-nonyl acridine orange, MitoFluor Green, and MitoTracker Green is affected by mitochondrial membrane potential altering drugs. *Cytometry*, 39, 203-10.
- Korke, R., M. L. Gatti, A. Lau, J. Lim, T. Seow, M. Chung & W. Hu (2004) Large scale gene expression profiling of metabolic shift of mammalian cells in culture. *J Biotechnol*, 107, 1-17.
- Maiorella, B. 1992. In vitro management of ammonia's effect on glycosylation of cell products through pH control. US Patent 5,096,816.

- Salvioli, S., A. Ardizzoni, C. Franceschi & A. Cossarizza (1997) JC-1, but not DiOC6(3) or rhodamine 123, is a reliable fluorescent probe to assess delta psi changes in intact cells: implications for studies on mitochondrial functionality during apoptosis. *FEBS Lett*, 411, 77-82.
- Subramanian, A., P. Tamayo, V. Mootha, S. Mukherjee, B. Ebert, M. Gillette, A. Paulovich, S. Pomeroy, T. Golub, E. Lander & J. Mesirov (2005) Gene set enrichment analysis: a knowledge-based approach for interpreting genome-wide expression profiles. *Proc Natl Acad Sci U S A*, 102, 15545-50.
- Swanson, K. & R. Hohl (2006) Anti-cancer therapy: targeting the mevalonate pathway. *Curr Cancer Drug Targets*, 6, 15-37.
- Trummer, E., K. Fauland, S. Seidinger, K. Schriebl, C. Lattenmayer, R. Kunert, K. Vorauer-Uhl, R. Weik, N. Borth, H. Katinger & D. Müller (2006) Process parameter shifting: Part I. Effect of DOT, pH, and temperature on the performance of Epo-Fc expressing CHO cells cultivated in controlled batch bioreactors. *Biotechnol Bioeng*, 94, 1033-44.
- Valley, U., M. Nimtz, H. Conradt & R. Wagner (1999) Incorporation of ammonium into intracellular UDP-activated N-acetylhexosamines and into carbohydrate structures in glycoproteins. *Biotechnol Bioeng*, 64, 401-17.
- Wood, I. & P. Trayhurn (2003) Glucose transporters (GLUT and SGLT): expanded families of sugar transport proteins. *Br J Nutr*, 89, 3-9.